



Published in final edited form as:

Nat Commun. 2013 ; 4: 2935. doi:10.1038/ncomms3935.

## Tumor-Associated Mutant p53 Drives the Warburg Effect

Cen Zhang<sup>1,5</sup>, Juan Liu<sup>1,5</sup>, Yingjian Liang<sup>2,3,5</sup>, Rui Wu<sup>1</sup>, Yuhan Zhao<sup>1,2</sup>, Xuehui Hong<sup>2,3</sup>, Meihua Lin<sup>1</sup>, Haiyang Yu<sup>1,2</sup>, Lianxin Liu<sup>3</sup>, Arnold J. Levine<sup>4</sup>, Wenwei Hu<sup>1,2,6</sup>, and Zhaohui Feng<sup>1,6</sup>

<sup>1</sup>Department of Radiation Oncology, Rutgers Cancer Institute of New Jersey, Rutgers, State University of New Jersey, New Brunswick, NJ 08902, USA

<sup>2</sup>Department of Pediatrics, Rutgers Cancer Institute of New Jersey, Rutgers, State University of New Jersey, New Brunswick, NJ 08902, USA

<sup>3</sup>Laboratory of Hepatosplenic Surgery, First Affiliated Hospital of Harbin Medical University, Harbin 150086, China

<sup>4</sup>The Institute for Advanced Study, Princeton, NJ 08540, USA

### Abstract

Tumor cells primarily utilize aerobic glycolysis for energy production, a phenomenon known as the Warburg effect. Its mechanism is not well-understood. The tumor suppressor gene *p53* is frequently mutated in tumors. Many tumor-associated mutant *p53* (mutp53) proteins not only lose tumor suppressive function, but also gain new oncogenic functions that are independent of wild type *p53*, defined as mutp53 gain-of-function (GOF). Here we show that tumor-associated mutp53 stimulates the Warburg effect in cultured cells and *mutp53* knock-in mice as a new mutp53 GOF. Mutp53 stimulates the Warburg effect through promoting GLUT1 translocation to plasma membrane, which is mediated by the activated RhoA and its downstream effector ROCK. Inhibition of the RhoA/ROCK/GLUT1 signaling largely abolishes mutp53 GOF in stimulating the Warburg effect. Furthermore, inhibition of glycolysis in tumor cells greatly compromises mutp53 GOF in promoting tumorigenesis. Thus, our results reveal a new mutp53 GOF and a mechanism for controlling the Warburg effect.

### Introduction

Tumor suppressor *p53* plays a central role in tumor prevention<sup>1–3</sup>. *p53* is the most frequently-mutated gene in human tumors. Majority of *p53* mutations, including several “mutational hotspots” in tumors (e.g. R175H, R248Q, and R273H), are missense mutations,

Users may view, print, copy, download and text and data- mine the content in such documents, for the purposes of academic research, subject always to the full Conditions of use: [http://www.nature.com/authors/editorial\\_policies/license.html#terms](http://www.nature.com/authors/editorial_policies/license.html#terms)

<sup>6</sup>Correspondence should be addressed to W. Hu (wh221@cinj.rutgers.edu) or Z. Feng. (fengzh@cinj.rutgers.edu).

<sup>5</sup>These authors contributed equally to this work.

#### Author contributions

Z. F., W.H. designed experiments. C. Z., Y.L., J.L., R.W., Y. Z. X.H. M.L. and H. Y. carried out the experiments. Z.F., W.H., C.Z., J.L., L.L., A.L. analyzed the data. Z. F. W.H. wrote the manuscript.

#### Conflict of interests

The authors declare no competing financial interests.

which usually result in the expression of full-length mutant p53 (mutp53) proteins in tumor cells. Recent studies have demonstrated that many tumor-associated mutp53 proteins, particularly these several “tumor hotspot mutants”, not only lose tumor suppressive functions of wild type p53 (wtp53), but also gain new oncogenic functions that are independent of wtp53, including promoting cell proliferation, anti-apoptosis and metastasis, which are defined as mutp53 gain-of-function (GOF) <sup>4-7</sup>. The mutp53 GOF is clearly demonstrated by *mutp53* knock-in mouse models; mice that express R172H or R270H mutp53 (equivalent to human R175H and R273H, respectively) develop an altered spectrum of tumors and more metastatic tumors compared with *p53*<sup>-/-</sup> mice <sup>8,9</sup>. The mechanism of mutp53 GOF in tumorigenesis is not well-understood.

Recent studies have shown that metabolic changes are a hallmark of tumor cells and a key contributor to tumor development <sup>10-13</sup>. The Warburg effect (or aerobic glycolysis) is the best characterized metabolic change in tumor cells. Most tumor cells primarily utilize glycolysis for their energy needs even under normal oxygen concentrations, a phenomenon termed “the Warburg effect” <sup>14</sup>. The Warburg effect is characterized by a much higher rate of glucose uptake and higher lactate production in tumor cells compared with normal cells <sup>10, 12-14</sup>. The Warburg effect provides a rationale for Positron Emission Tomography imaging developed for tumor detection since tumors take up more of the glucose analog <sup>18</sup>fluorodeoxyglucose than normal tissues. Emerging evidence has indicated that the Warburg effect contributes greatly to tumorigenesis and could be targeted for tumor therapy <sup>12, 15, 16</sup>. However, the mechanism for the Warburg effect is not well-understood.

As a transcription factor, wtp53 mainly exerts its function in tumor suppression through transcriptional regulation of its target genes to initiate various cellular responses, including cell cycle arrest and apoptosis <sup>1-3</sup>. Recent studies have shown that regulating energy metabolism is a critical function of wtp53 in tumor suppression <sup>12, 13, 17, 18</sup>. Wtp53 represses glycolysis and the Warburg effect through transcriptional regulation of genes involved in energy metabolism, including *SCO2*, *TIGAR*, *GLS2* and *Parkin* <sup>19-22</sup>. Loss of wtp53 leads to the Warburg effect in cultured cells and mice. It remains unknown whether mutp53 can stimulate the Warburg effect as a novel GOF.

In this study, we find that tumor-associated mutp53 stimulates the Warburg effect both in cultured cells and *mutp53* knock-in mice. This effect is mainly through promoting the translocation of GLUT1 (glucose transporter 1) to plasma membrane, which is mediated by an activated RhoA/ROCK signaling. Inhibition of glycolysis and the Warburg effect in tumor cells greatly attenuates mutp53 GOF in tumorigenesis. Our results demonstrate a new mutp53 GOF, and also reveal a mechanism for the Warburg effect in cancer cells.

## Results

### Mutp53 stimulates the Warburg Effect *in vitro* and *in vivo*

The Warburg effect is characterized by greatly increased glucose uptake and lactate production in tumor cells <sup>12, 14</sup>. To investigate the effect of mutp53 on the Warburg effect, p53-null human lung carcinoma H1299 cells were stably transduced with retroviral vectors expressing “tumor hotspot mutants” R175H, R248Q and R273H mutp53, respectively, and

the levels of glucose uptake, glycolytic rate and lactate production in cells were measured. Expression of R175H, R248Q and R273H mutp53 in H1299 cells greatly stimulated the Warburg effect; much higher levels of glucose uptake, glycolytic rate and lactate production were observed in cells with mutp53 expression compared with control cells (Fig. 1a). A similar effect was observed for endogenous mutp53; in human breast SK-BR3 and MDA-MB468 cells which express R175H and R273H mutp53, respectively, knockdown of endogenous mutp53 by shRNA vectors greatly reduced glucose uptake, glycolytic rate and lactate production (Fig. 1b). This stimulating effect of mutp53 on the Warburg effect was also observed in mouse embryonic fibroblasts (MEFs) from  $p53^{R172H/R172H}$  knock-in mice (equivalent to human *R175H*). Compared with  $p53^{-/-}$  MEFs,  $p53^{R172H/R172H}$  MEFs showed clearly enhanced glucose uptake, glycolytic rate and lactate production (Fig. 1c). Furthermore, the enhanced glucose uptake was observed in different tissues in  $p53^{R172H/R172H}$  mice compared with  $p53^{-/-}$  mice, including the liver, lung and small intestine (Fig. 1d). It is well-established that the serum lactate level indicates glycolytic status in mice<sup>23, 24</sup>.  $p53^{R172H/R172H}$  mice showed much higher levels of serum lactate than  $p53^{-/-}$  mice (Fig. 1e), indicating a higher glycolytic rate in  $p53^{R172H/R172H}$  mice.

Recently, wtp53 was reported to repress the Warburg effect<sup>19–21</sup>. To further confirm that this stimulating effect of mutp53 on the Warburg effect is a novel mutp53 GOF and is independent of the function of wtp53, we examined whether wtp53 exhibits an inhibitory effect on the Warburg effect as reported using our systems. As shown in Fig. 2a,  $p53^{+/+}$  MEFs displayed much lower levels of glucose uptake, glycolytic rate and lactate production than  $p53^{-/-}$  MEFs. Consistently, compared with  $p53^{-/-}$  mice,  $p53^{+/+}$  mice displayed a much lower level of glucose uptake in different tissues (Fig. 2b), and a clear lower level of serum lactate (Fig. 2c). Furthermore, knockdown of endogenous wtp53 by shRNA vectors in human breast MCF7, lung H460 and A549 cells clearly promoted the glucose uptake, glycolytic rate and lactate production compared with control cells transduced with control shRNA vectors (Fig. 2d). These results clearly show that wtp53 can repress the Warburg effect *in vitro* and *in vivo*, which is consistent with previous reports<sup>19–21</sup>. Thus, our results clearly demonstrate that stimulating the Warburg effect is a novel mutp53 GOF, which is independent of wtp53's function.

### Mutp53 promotes GLUT1 translocation

Transport of glucose across the plasma membrane (PM) of cells is the first rate-limiting step for glucose metabolism, which is mediated by glucose transporters (GLUTs), including GLUT1-4. GLUT4 is the main glucose transporter expressed in insulin-responsive fat and muscle tissues. Insulin dramatically stimulates the translocation of GLUT4 to the PM to promote the glucose uptake in fat and muscle. GLUT1-3 are responsible for the basal glucose uptake in cells and tissues<sup>25</sup>. Among them, GLUT1 is widely expressed in almost all types of cells and tissues and responsible for their basal glucose uptake, whereas GLUT2 and 3 are responsible for the basal glucose uptake in some specific tissues<sup>25</sup>. While the dysregulation of GLUT4 signaling is an important cause for type 2 diabetes, dysregulation of GLUT1-3 signaling, especially GLUT1, contributes to tumorigenesis. For example, GLUT1 is frequently overexpressed in tumors, which contributes to the Warburg effect<sup>26, 27</sup>. Indeed, ectopic expression of GLUT1 by expression vectors in H1299 and

*p53*<sup>-/-</sup> MEF cells greatly enhanced glucose uptake, glycolytic rate and lactate production in cells (Supplementary Fig. S1a–d). It has been well-established that increased translocation of GLUT1 from the intracellular pool to the PM promotes glucose transport<sup>25, 28</sup>. Interestingly, mutp53 promoted GLUT1 translocation to the PM in cells. Ectopic expression of mutp53 greatly increased GLUT1 levels on the PM but did not change the total GLUT1 levels in H1299 cells as measured by Western-blot assays using isolated PM fractions (Fig. 3a). To confirm this result, cells were transduced with pLPCX-Myc-GLUT1 vectors expressing GLUT1 with Myc tag in its first exofacial loop, and the levels of Myc-GLUT1 on the cell surface or in the whole cell were measured by immunofluorescence (IF) staining with an anti-Myc antibody followed by flow cytometry analysis. Mutp53 clearly increased the levels of Myc-GLUT1 protein on the PM but did not affect the total Myc-GLUT1 levels in H1299 cells (Fig. 3b). Similar results were observed by IF staining of cells transduced with pLPCX-Myc-GLUT1 vectors; mutp53 expression in H1299 clearly promoted the translocation of Myc-GLUT1 protein from cytoplasm to the cell surface (Fig. 3c). Furthermore, knockdown of endogenous mutp53 in SK-BR3 and MDA-MB468 cells clearly reduced the levels of endogenous GLUT1 on the PM but not the total GLUT1 levels in the cells as analyzed by Western-blot assays (Fig. 3d), and reduced the levels of exogenous Myc-GLUT1 on the PM but not the total Myc-GLUT1 levels in the cells as analyzed by IF assays in a flow cytometry (Fig. 3e). IF staining showed that mutp53 knockdown in both cell lines clearly decreased Myc-GLUT1 distribution on cell surface and increased its distribution in cytoplasm (Fig. 3f).

Consistent results were observed in *p53*<sup>R172H/R172H</sup> MEF cells; R172H mutp53 clearly promoted the translocation of GLUT1 of both endogenous GLUT1 and Myc-GLUT1 in MEF cells (Fig. 3g & h). Similar results were observed in *p53*<sup>R172H/R172H</sup> mice; compared with *p53*<sup>-/-</sup> mice, mutp53 clearly increased GLUT1 levels on the PM but not the total GLUT1 levels in different tissues from *p53*<sup>R172H/R172H</sup> mice, including the liver (Fig. 3i), lung and small intestine tissues (Supplementary Fig. S2).

Interestingly, mutp53 did not affect the translocation of GLUT2 or GLUT3, the other two glucose transporters that regulate the basal glucose uptake in certain types of tissues and cells. Expression of R175H, R248Q or R273H mutp53 in H1299 cells or R172H mutp53 in *p53*<sup>R172H/R172H</sup> MEFs did not affect the levels of endogenous GLUT2/3 or Myc-GLUT2/3 on the PM or in the whole cell compared with control H1299 cells and *p53*<sup>-/-</sup> MEFs cells, respectively (Fig. 3j & k). The expression of GLUT4 and its translocation to the PM were also examined in H1299 and *p53*<sup>R172H/R172H</sup> MEF cells. The levels of GLUT4 were too low to be detected in these two cell lines (Fig. 3j), indicating that GLUT4 is not a major contributor to the role of mutp53 in stimulating the Warburg effect in these cells.

To test whether the enhanced GLUT1 translocation mediates the stimulating effect of mutp53 on the Warburg effect, endogenous GLUT1 was knocked down by shRNA in cells. While GLUT1 overexpression promotes the Warburg effect (Supplementary Fig. S1), GLUT1 knockdown clearly reduced the glucose uptake, glycolytic rate and lactate production in H1299 and MEF cells (Fig. 4a & b). Notably, GLUT1 knockdown largely abolished the stimulating effect of mutp53 on the Warburg effect in H1299 cells and in *p53*<sup>R172H/R172H</sup> MEF cells (Fig. 4a & b). In SK-BR3 and MDA-MB468 cells, GLUT1

knockdown clearly reduced the Warburg effect, similar to the effect of mutp53 knockdown (Fig. 4c). However, simultaneous knockdown of mutp53 and GLUT1 in these two cell lines did not produce additive inhibitory effect on the Warburg effect (Fig. 4c), further suggesting that GLUT1 mediates the stimulating effect of mutp53 on the Warburg effect in cells.

Similar to the effect of GLUT1 knockdown on the Warburg effect, knockdown of endogenous GLUT3 by shRNA vectors in H1299 and MEFs greatly reduced glucose uptake, glycolytic rate and lactate production to similar levels as that resulted from GLUT1 knockdown (Fig. 4d & e). However, GLUT3 knockdown did not clearly affect the promoting effect of mutp53 on the Warburg effect, which was still clearly observed in both cell lines with lower glycolytic rates caused by GLUT3 knockdown (Fig. 4d & e). Similarly, knockdown of GLUT2 clearly reduced the Warburg effect in *p53<sup>R172H/R172H</sup>* MEFs, but did not clearly affect the promoting effect of mutp53 on the Warburg effect (Fig. 4e). These results strongly suggest that the promoting effect of mutp53 on the Warburg effect is mediated by GLUT1. Taken together, these results indicate that mutp53 can specifically promote GLUT1 translocation to the PM, which is an important mechanism for mutp53 to stimulate the Warburg effect in tumor cells.

### Mutp53 stimulates the Warburg effect through RhoA activation

Small GTPase proteins, such as Rab and Rho families, were reported to be involved in the regulation of insulin-stimulated GLUT4 translocation to the PM and insulin-stimulated glucose uptake in fat and muscle, two insulin responsive tissues<sup>25, 29</sup>. RhoA is a small GTPase that belongs to the Rho family. RhoA is frequently overexpressed or activated in tumors and contributes to tumorigenesis by promoting proliferation and metastasis of tumor cells<sup>30, 31</sup>. RhoA is also involved in stimulating GLUT4 translocation to the PM in response to insulin stimulation in fat and muscle cells<sup>32, 33</sup>. Interestingly, mutp53 was recently reported to activate RhoA through its up-regulation of the expression of positive regulators for RhoA, including RhoGDI and Rho GEF-H1<sup>34–37</sup>. These findings raised a possibility that mutp53 may promote GLUT1 translocation and stimulate the Warburg effect through its activation of RhoA in tumor cells. However, the translocation regulation of GLUT1 and GLUT4 in cells is quite different, which is highly cell-type specific<sup>25, 32</sup>. For example, the translocation of GLUT4 is dramatically stimulated by insulin, whereas GLUT1 translocation is not markedly regulated by insulin<sup>25, 32</sup>. Currently, it is unclear whether RhoA can regulate GLUT1 translocation to affect the basal glucose uptake, and whether RhoA activation can promote the Warburg effect in cancer cells.

We first tested whether mutp53 activates RhoA in the cells we used for this study. RhoA cycles between inactive GDP-bound and active GTP-bound states in cells<sup>31, 38</sup>. As shown in Fig. 5a, expression of mutp53 greatly increased the levels of RhoA-GTP but not the total RhoA in H1299 and *p53<sup>R172H/R172H</sup>* MEF cells, and furthermore, knockdown of endogenous mutp53 greatly reduced the levels of RhoA-GTP but not the total RhoA in MDA-MB468 and SK-BR3 cells. We further investigated whether RhoA activation promotes GLUT1 translocation and the Warburg effect, and whether RhoA activation mediates mutp53's GOF in stimulating the Warburg effect in cancer cells. Ectopic expression of RhoA by vectors in H1299 and *p53*<sup>-/-</sup> MEF cells greatly promoted the

translocation of GLUT1 (Fig. 5b) to the PM, and furthermore, greatly stimulated the Warburg effect (Fig. 5c). Consistently, RhoA knockdown by shRNA vectors or siRNA oligos clearly reduced the translocation of endogenous GLUT1 (Fig. 5d) and Myc-GLUT1 to the PM (Fig. 5e–g), and reduced the Warburg effect (Fig. 5h–j) in H1299, MDA-MB468 and *p53*<sup>R172H/R172H</sup> MEF cells. Importantly, RhoA knockdown largely abolished the promoting effects of mutp53 on GLUT1 translocation to the PM (Fig. 5d–g) and the Warburg effect (Fig. 5h–j) in these cells. Similar results were observed in SK-BR3 cells (Supplementary Fig. S3a–c). Interestingly, consistent with the effect of mutp53 on GLUT2 and 3, RhoA did not show clear effect on the translocation of GLUT2 or 3 to the PM (Supplementary Fig. S4). These results together clearly demonstrate a novel function of RhoA in tumorigenesis; RhoA activation promotes GLUT1 translocation to the PM, and therefore, promotes the Warburg effect in cancer cells, which is an important mechanism for mutp53 to stimulate the Warburg effect in cancer cells.

### ROCK mediates the effect of mutp53

RhoA has been reported to regulate many proteins and different signaling pathways. Among them, ROCK (Rho-associated protein kinase) is a direct downstream effector kinase of RhoA. ROCK has two isoforms, ROCK1 and ROCK2 (ROCK1/2)<sup>30, 38</sup>. ROCK has been reported to regulate insulin-stimulated GLUT4 translocation and glucose uptake in fat and muscle tissues<sup>39–41</sup>. However, since the translocation regulation of GLUT1 and GLUT4 in cells is quite different and highly cell-type specific<sup>25, 32</sup>, it is unclear whether ROCK activation can promote GLUT1 translocation and the Warburg effect in cancer cells.

We investigated whether ROCK mediates mutp53 GOF in stimulating the Warburg effect. MYPT1 (myosin phosphatase target subunit 1) and MLC2 (myosin light chain 2) are two well-known downstream targets of ROCK, which can be phosphorylated by ROCK at Thr696 and Ser19, respectively<sup>30, 38</sup>. First, we examined whether mutp53 enhances the activities of ROCK1/2 in cells by measuring the levels of phosphorylation at Thr696 of MYPT1 using enzyme immunoassays. Expression of mutp53 enhanced ROCK1/2 activities in H1299 and MEF cells, whereas knockdown of mutp53 reduced the ROCK1/2 activities in SK-BR3 and MDA-MB468 cells (Fig. 6a). This result was confirmed by Western-blot assays showing that mutp53 expression clearly increased the phosphorylation of MYPT1 at Thr696 and MLC2 at Ser19 in H1299 cells (Supplementary Fig. S5a), whereas knockdown of endogenous mutp53 clearly reduced phosphorylation in MDA-MB468 cells (Supplementary Fig. S5b). This effect of mutp53 was largely abolished when RhoA or ROCK1/2 was knocked down by shRNA vectors or siRNA oligos (Supplementary Fig. S5a–d), indicating the mutp53 regulates the phosphorylation of MYPT1 and MLC2 through activation of the RhoA/ROCK signaling.

We further tested whether ROCK activation promotes GLUT1 translocation and the Warburg effect in cancer cells, and whether ROCK activation mediates mutp53's role in stimulating GLUT1 translocation and the Warburg effect. Y27632, a widely-used inhibitor for ROCK1/2<sup>30, 38, 42</sup>, was employed to block ROCK1/2 activities in cells. Y27632 clearly reduced ROCK activities represented by the reduced phosphorylation of MYPT1 at Thr696 and MLC2 at Ser19 as measured by enzyme immunoassays and Western-blot assays

(Supplementary Fig. S5e & f). Furthermore, Y27632 largely abolished the promoting effect of mutp53 on ROCK activities in cells (Supplementary Fig. S5e & f). Notably, Y27632 greatly reduced the translocation of GLUT1 to the PM (Fig. 6b & c), and the Warburg effect in H1299 cells (Fig. 6d). Consistent results were observed in *p53<sup>R172H/R172H</sup>* MEF cells (Fig. 6b, e & f). Importantly, Y27632 largely abolished the promoting effects of mutp53 on the translocation of GLUT1 to the PM (Fig. 6b, c & e), and the Warburg effect in these cells (Fig. 6d & f). Consistent results were observed in both SK-BR3 and MDA-MB468 cells (Supplementary Fig. S6).

To further confirm that the role of ROCK in mediating the mutp53's effect on GLUT1 translocation and the Warburg effect, the endogenous ROCK1/2 were knocked down by siRNA oligos. Consistent with the results of Y27632 treatments, knockdown of ROCK1/2 greatly reduced the GLUT1 translocation and the Warburg effect in cells, and furthermore, largely abolished the stimulating effects of mutp53 on GLUT1 translocation and the Warburg effect in H1299 (Fig. 6c & d), *p53<sup>R172H/R172H</sup>* MEF (Fig. 6e & f) and MDA-MB468 cells (Supplementary Fig. S6c & e). These results clearly show that as a downstream effector of RhoA, ROCK mediates mutp53's role in stimulating GLUT1 translocation and the Warburg effect in cancer cells.

The PI3K/AKT and ERK pathways, two pathways that are frequently activated in cancer, were reported to promote glucose uptake in cells<sup>43-45</sup>. To investigate whether these two pathways contribute to the promoting effects of mutp53 on the Warburg effect, we first examined whether mutp53 can activate these two pathways in these cell lines that we employed for this study by measuring the levels of phosphorylation of AKT at Thr473 and phosphorylation of ERK1/2 at Thr202/Tyr204, respectively. Mutp53 slightly increased the AKT activity in H1299 cells, which is consistent with a previous report<sup>5</sup>, but not in MDM-MB468 or MEF cells, suggesting that the activation of AKT by mutp53 is cell type- and context-dependent (Supplementary Fig. S7a)<sup>46</sup>. Mutp53 showed no clear effect on the ERK signaling in these cell lines (Supplementary Fig. S7b). To further test whether blocking the AKT and ERK signaling pathways affect the role of mutp53 in the Warburg effect, H1299 cells with or without mutp53 expression were treated with PI3K/AKT inhibitors, Wortmannin and LY294002<sup>43, 45</sup>, or ERK inhibitors, U0126 and PD98059<sup>44</sup>, and their impacts upon mutp53's effect on glucose uptake were examined. All these treatments greatly reduced the glucose uptake in H1299 cells. However, these treatments did not clearly affect the promoting effects of mutp53 on glucose uptake (Supplementary Fig. S7c & d). These results strongly suggested that the PI3K/AKT and ERK signaling pathways did not contribute significantly to the promoting effect of mutp53 on the Warburg effect in these cells.

Insulin/IGF-1 (insulin-like growth factor-1) signaling plays an important role in the regulation of the translocation of glucose transporters and glucose uptake in insulin-responsive muscle and fat tissues<sup>25</sup>. Activated IGF-1/IGF-1 receptor signaling also plays an important role in cancer<sup>47</sup>. To investigate whether the activated insulin/IGF-1 signaling contributes to the effect of mutp53 on the GLUT1 translocation, H1299 cells were treated with insulin and IGF-1, respectively, to activate the insulin/IGF-1 signaling. Both insulin and IGF-1 moderately induced the GLUT1 protein expression (by ~2-fold at 8 h after

treatments), and furthermore, slightly promoted GLUT1 translocation to the PM (by ~20–30% at 10 min, 4 and 8 h after treatments) in H1299 cells (Supplementary Fig. S8). However, these effects were not mutp53-specific since similar effects were observed in both H1299 cells with or without mutp53 expression. Furthermore, the effect of insulin and IGF-1 on GLUT1 translocation was much weaker compared with the effect of mutp53. These results suggested that activated insulin/IGF-1 signaling did not contribute significantly to the effect of mutp53 on GLUT1 translocation in H1299 cells.

### **Mutp53 stimulates the Warburg effect via RhoA/ROCK *in vivo***

We further investigated whether mutp53 stimulates the Warburg effect through the activation of the RhoA/ROCK signaling *in vivo* as what we observed in cultured cells. Indeed, the stimulating effect of mutp53 on the activities of RhoA and ROCK were also observed in *p53*<sup>R172H/R172H</sup> mice. Compared with *p53*<sup>-/-</sup> mice, much higher levels of RhoA-GTP (Fig. 6g) and ROCK activities (Fig. 6h; Supplementary Fig. S9) were observed in different tissues of *p53*<sup>R172H/R172H</sup> mice, including the liver, lung and small intestine. Treating mice with Y27632 (i.p. injection) clearly reduced the GLUT1 translocation to the PM (Fig. 6i) and glucose uptake (Fig. 6j) in different tissues, and serum lactate levels (Fig. 6k). Importantly, Y27632 largely abolished mutp53's effects on ROCK activation (Supplementary Fig. S9), GLUT1 translocation (Fig. 6i), glucose uptake (Fig. 6j), and serum lactate levels (Fig. 6k). These results clearly show that the activated RhoA/ROCK signaling mediates the promoting effect of mutp53 on GLUT1 translocation and the Warburg effect *in vivo*.

### **Mutp53 enhances actin polymerization**

Rho family proteins, including RhoA, induce actin polymerization and play an important role in vesicular trafficking, which is critical for the translocation of glucose transporters<sup>29, 48, 49</sup>. Actin polymerization, the assembly of actin monomers into filaments (polymeric actin or F-actin), plays a critical role in vesicular trafficking<sup>29, 48, 49</sup>. ROCK has been reported to regulate insulin-stimulated GLUT4 translocation and glucose uptake in fat and muscle through the regulation of actin polymerization<sup>39</sup>. Interestingly, we found that mutp53 promoted actin polymerization. Expression of mutp53 clearly increased the levels of polymeric actin but not total actin in H1299 cells (Fig. 7a). This effect of mutp53 on actin polymerization can be largely abolished by inhibition of RhoA/ROCK signaling, including RhoA knockdown and Y27632 treatments (Fig. 7a). Cytochalasin D and latrunculin B, two widely-used actin polymerization inhibitors<sup>50, 51</sup>, which abolished the promoting effect of mutp53 on actin polymerization (Fig. 7b), also largely abolished the stimulating effects of mutp53 on the translocation of endogenous GLUT1 (Fig. 7c) and Myc-GLUT1 (Fig. 7d) to the PM in H1299 cells. Most importantly, cytochalasin D and latrunculin B largely abolished the stimulating effects of mutp53 on the Warburg effect in H1299 cells (Fig. 7e). These results were confirmed in *p53*<sup>R172H/R172H</sup> MEF (Fig. 7f–h) and MDA-MB468 cells (Fig. 7i–k). These results strongly suggest that mutp53 can enhance actin polymerization through activating RhoA/ROCK signaling, which is one of the mechanisms that leads to the enhanced GLUT1 translocation to the PM and the Warburg effect in cancer cells.

## Mutp53 GOF in the Warburg effect promotes tumorigenesis

The Warburg effect has been recently demonstrated as a key contributor to tumor progression, and reversing the Warburg effect greatly compromised tumorigenicity of tumor cells<sup>12, 15, 16</sup>. We investigated whether stimulating the Warburg effect is an important mechanism contributing to mutp53's role in tumorigenesis. Consistent with the reported GOF of mutp53 in tumorigenesis<sup>4-7</sup>, mutp53 promoted tumorigenesis in H1299 and MDA-MB468 cells. Expression of R175H, R248Q, or R273H mutp53 in H1299 cells clearly promoted the anchorage-independent growth of the cells on soft agar (Fig. 8a), whereas knockdown of endogenous R273H mutp53 in MDA-MB468 cells clearly reduced the anchorage-independent growth of the cells (Fig. 8b). Furthermore, expression of mutp53 in H1299 cells clearly promoted the growth of xenograft tumors formed by H1299 cells in nude mice (Fig. 8c-e), whereas knockdown of endogenous R273H mutp53 in MDA-MB468 cells clearly reduced the growth of xenograft tumors formed by MDA-MB468 cells (Fig. 8f). Notably, knockdown of GLUT1 or RhoA by shRNA largely abolished the promoting effects of mutp53 on both anchorage-independent growth (Fig. 8a & b) and xenograft tumor growth (Fig. 8c-f) in H1299 and MDA-MB468 cells.

To further test this hypothesis, cells were cultured in media containing galactose instead of glucose to inhibit glycolysis<sup>52, 53</sup> for anchorage-independent growth assays. Galactose enters glycolysis through the Leloir pathway, which occurs at a much lower rate than glucose entry into glycolysis. Consistent with previous reports<sup>53</sup>, galactose greatly reduced the anchorage-independent growth in H1299 (Fig. 8g) and MDA-MB468 cells (Fig. 8h). Notably, galactose largely abolished the promoting effect of mutp53 on the anchorage-independent growth in H1299 cells (Fig. 8g) and MDA-MB468 cells (Fig. 8h). Taken together, these results clearly show that inhibition of the Warburg effect or glycolysis greatly compromised mutp53 GOF in promoting tumorigenesis, and strongly suggest that mutp53 GOF in stimulating the Warburg effect promotes tumorigenesis.

## Discussion

Recent studies have demonstrated that many tumor-associated mutp53 proteins gain new oncogenic functions to promote tumor cell proliferation, anti-apoptosis, metastasis and lipid metabolism<sup>4-7</sup>. However, the mechanism of mutp53 GOF in tumorigenesis is not well-understood. Results from this study clearly demonstrate a novel GOF of mutp53 in both cultured cells and *mutp53* knock-in mice, i.e. mutp53 stimulates the Warburg effect. This function of mutp53 is contrary to the function of wtp53 in repressing the Warburg effect, which was confirmed by our results in this study (Fig. 1&2). Mutp53 does not affect the expression of GLUT1, but promotes GLUT1 translocation to the PM. GLUT1 knockdown largely abolishes this stimulating effect of mutp53 on the Warburg effect in cells. Furthermore, mutp53 does not affect the expression or the PM translocation of GLUT2 or GLUT3. Knockdown of GLUT2 or GLUT3 clearly reduced the Warburg effect in cells, but did not clearly affect the stimulating effect of mutp53 on the Warburg effect. Currently, the mechanism by which mutp53 specifically regulates the translocation of GLUT1 in tumor cells remains unclear. These results strongly suggest that promoting the GLUT1

translocation to the PM is an important mechanism by which mutp53 stimulates the Warburg effect.

GLUTs, including GLUT1-4, mediate the transport of glucose across the PM, a critical step for glucose metabolism. Each of these GLUTs displays distinct expression patterns in cells and tissues. For example, GLUT4 is specifically and highly expressed in fat and muscle tissues, and is responsive to insulin-stimulated glucose uptake in these two tissues. In contrast, GLUT1 is ubiquitously expressed and responsible for the basal glucose uptake in various types of cells. The regulation of GLUTs translocation is different among GLUTs, and the mechanisms appear to be highly cell type- and context-dependent<sup>25, 32</sup>. For example, while translocation of GLUT4 is dramatically stimulated by insulin in fat and muscle cells, the translocation of GLUT1 is not markedly regulated by insulin<sup>25, 32</sup>. It has been reported that the RhoA/ROCK signaling is involved in the regulation of the insulin-stimulated translocation of GLUT4 and glucose uptake<sup>25, 32, 33, 40</sup>. However, it is unclear whether RhoA/ROCK signaling can regulate GLUT1 translocation and the basal glucose uptake in cells, especially in cells other than fat and muscle. Furthermore, it is unclear whether RhoA/ROCK activation in cancer cells promotes the Warburg effect in cancer cells. Results from this study clearly show that RhoA/ROCK can promote the translocation of GLUT1 to the PM and promote the basal glucose uptake in various cells. Furthermore, the activation of RhoA/ROCK signaling by mutp53 mediates mutp53's role in promoting GLUT1 translocation and the Warburg effect in cancer cells. Inhibition of RhoA/ROCK signaling by knocking down RhoA or ROCK1/2, or by the ROCK inhibitor Y27632 all largely abolishes the stimulating effect of mutp53 on the GLUT1 translocation to the PM and the Warburg effect in cells. Thus, our results reveal that promoting the GLUT1 translocation to the PM to stimulate the Warburg effect in cancer cells is a novel mechanism by which the activated RhoA/ROCK signaling promotes tumorigenesis, especially in cells containing mutp53.

The RhoA signaling is frequently activated in many types of cancer, which plays a critical role in promoting tumor cell proliferation, invasion and metastasis<sup>30, 31</sup>. In addition to our finding that mutp53 promotes the Warburg effect through RhoA activation, recent studies also showed that the activation of RhoA by mutp53 contributes to the GOF of mutp53 in tumor proliferation, invasion and metastasis<sup>34-37</sup>. These findings together indicate an important role of the RhoA signaling in mediating mutp53 GOF in cancer. However, it is still not well-understood how mutp53 activates RhoA. As a small GTPase, RhoA activity is regulated by many positive and negative regulators, especially a group of Rho GEFs, Rho GAPs, and Rho GDIs. Recently, it was reported that mutp53 activates RhoA through transcriptional up-regulation of RhoGDI and Rho GEF-H1, two positive regulators for RhoA<sup>34-36</sup>. It will be of interest to examine whether mutp53 can regulate the expression of some other RhoA regulators to activate RhoA, including up-regulation of additional positive regulators and/or down-regulation of some negative regulators for RhoA. In addition to the transcription regulation, mutp53 can interact with other proteins to affect their functions, which contributes to the GOF of mutp53 in cancer<sup>6, 54</sup>. It is possible that mutp53 interacts with some upstream regulators for RhoA to activate RhoA. Considering the important role of mutp53/RhoA signaling in tumorigenesis and potential therapeutic applications, future studies are needed to elucidate the molecular mechanism by which mutp53 activates RhoA.

In summary, our results clearly demonstrate that stimulating the Warburg effect in tumor cells is a novel GOF of tumor-associated mutp53. Our results also reveal that mutp53 acts as an important mediator for the Warburg effect in cancer cells, which provides a new mechanism for the Warburg effect. Emerging evidence has strongly suggested that as a hallmark of tumor cells, metabolic changes in tumors, such as the Warburg effect, could be targeted for tumor therapy. Our results strongly suggest that targeting altered glucose metabolism could be a feasible therapeutic strategy for tumor carrying mutp53.

## Methods

### Cells and vectors

H1299, SK-BR3, MDA-MB468, H460, MCF-7, and A549 cells were obtained from ATCC (Manassas, VA). The p53-null human lung H1299 cells were transduced with pLPCX-mutp53 retroviral vectors expressing R175H, R248Q and R273H mutp53, respectively, to establish cells with stable ectopic expression of mutp53. Human breast SK-BR3 cells expressing R175H mutp53 and MDA-MB468 cells expressing R273H mutp53 were transduced with shRNA vectors against p53 to establish cells with stable knockdown of endogenous mutp53<sup>21</sup>. pBABE-p53shRNA retroviral shRNA vectors against p53 was a generous gift from Dr. R. Agami (The Netherlands Cancer Institute). The lentiviral shRNA vector against p53 (TRCN0000003755) were purchased from Sigma. Control cells were transduced with empty vectors. *p53*<sup>-/-</sup> and *p53*<sup>R172H/R172H</sup> MEF cells were established following the published method<sup>55</sup>. RhoA expression vector pLPCX-Flag-RhoA was constructed by using Flag-RhoA DNA fragment from pCMV5-Flag-RhoA (Addgene). Lentiviral shRNA vectors against human GLUT1 (V3LHS\_321625 and V3LHS\_321626), human GLUT3 (V3LHS\_323130 and V3LHS\_323134) and human RhoA (V3LHS\_646048 and V3LHS\_642222) were purchased from Open Biosystems (Huntsville, AL). siRNA oligos against ROCK1 (for human: HSC.RNAI.N005406.12.1, and HSC.RNAI.N005406.12.2; for mouse: MMC.RNAI.N009071.12.1, and MMC.RNAI.N009071.12.3), ROCK2 (for human: HSC.RNAI.N004850.12.1, and HSC.RNAI.N004850.12.2; for mouse: MMC.RNAI.N009072.12.1, and MMC.RNAI.N009072.12.4), mouse GLUT1 (MMC.RNAI.N011400.12.4, and MMC.RNAI.N011400.12.5), mouse GLUT3 (MMC.RNAI.N011401.12.2, and MMC.RNAI.N011401.12.4) were purchased from Integrated DNA Technologies. siRNA oligos against mouse GLUT2 (5'-AAGUUGGAAGAGGAAGUCATT-3', and 5'-CGGAAAGCUGCCAUAACUTT-3') were synthesized by Sigma. To avoid off-target effects, two different shRNA vectors or siRNA oligos against each gene were employed. For treatment of ROCK inhibitor Y27632, cells were treated with Y27632 (5, 10, and 20  $\mu$ M; stock solution was prepared in H<sub>2</sub>O) for 6 h before assays. For treatments of AKT inhibitors, cells were treated with Wortmannin (0.5, 1, and 2  $\mu$ M) or LY249002 (10, 20, 30  $\mu$ M) for 3 h before assays. For treatments of ERK inhibitors, cells were treated with U0126 (0.5, 1 and 2  $\mu$ M) or PD98059 (5, 10 and 20  $\mu$ M) for 2 h before assays. For treatments of IGF-1 and insulin, cells were serum starved for 12 h before they were treated with IGF-1 (50 and 100 ng/ml) or insulin (50 and 100 nM) for 10 min, 4 h and 8 h before assays.

### **In vivo glucose uptake assays and serum lactate measurements**

Assays for glucose uptake in mouse tissues were performed as described<sup>56, 57</sup>. Briefly, five-week-old male *p53*<sup>+/+</sup>, *p53*<sup>-/-</sup> and *p53*<sup>R172H/R172H</sup> C57BL6/J mice<sup>8</sup> (generous gifts from Dr. Gigi Lozano) were injected (i.p.) with <sup>3</sup>H-2-deoxyglucose (1  $\mu$ ci/g body weight) and tissues were collected at 1.5 h after injection to measure the levels of <sup>3</sup>H-2-deoxyglucose-6-phosphate accumulated in tissues. To study the effect of ROCK inhibitor Y27632 on glucose uptake of tissues, mice were injected (i.p.) with Y27632 (10  $\mu$ g/g body weight) or PBS at 3 h before injection (i.p.) of <sup>3</sup>H-2-deoxyglucose. The lactate levels in serum were determined by using a lactate Assay Kit according to the manufacturer's instruction (Biovision). All mouse experiments were approved by the Institutional Animal Care and Use Committee of Rutgers University.

### **Measurements of glucose uptake in cells**

Glucose uptake was measured by measuring the uptake of <sup>3</sup>H-2-deoxyglucose by cells<sup>21, 58</sup>. Briefly, cells cultured in 12-well plates were pre-incubated in glucose-free media for 30 min. <sup>3</sup>H-2-deoxyglucose (1  $\mu$ Ci/well) was then added to the cells and incubated for 30 min before cells were washed with PBS and lysed in 1% SDS. The radioactivity of cell lysates was determined in a liquid scintillation counter and normalized to the protein concentrations of cell lysates.

### **Measurements of glycolytic rates in cells**

The glycolytic rate was measured by monitoring the conversion of 5-<sup>3</sup>H-glucose to <sup>3</sup>H-H<sub>2</sub>O<sup>19, 21</sup>. Briefly, cells ( $1 \times 10^6$ ) were washed in PBS and then resuspended in 1 mL of Krebs buffer without glucose for 30 min at 37 °C. Cells were then resuspended in 0.5 mL of Krebs buffer containing 10 mM glucose and 5  $\mu$ Ci of 5-[<sup>3</sup>H]glucose for 1 h. Triplicate 100  $\mu$ L aliquots were transferred to uncapped PCR tubes containing 100  $\mu$ L of 0.2 N HCl, and a tube was transferred to a scintillation vial containing 0.5 mL of H<sub>2</sub>O. The scintillation vials were sealed and left for 48 h to allow diffusion to occur. The amounts of diffused and undiffused <sup>3</sup>H were determined in a liquid scintillation counter.

### **Measurements of lactate production in cells**

Cells were cultured in fresh phenol red-free media and incubated for 12–24 h before the culture media were collected. The lactate levels were determined by using lactate Assay Kits according to the manufacturer's instruction (Biovision), and normalized with cell number<sup>21</sup>.

### **Western-blot Assays**

Standard Western blot assays and following antibodies were used to analyze protein expression. GLUT1 (Abcam; 1:4000); GLUT2 (Abcam; 1:2000); GLUT3 (Abcam; 1:2000); GLUT4 (Santa Cruz; 1:2000); RhoA (Millipore; 1:2000); p53 (Santa Cruz; 1:1000);  $\beta$ -actin (Sigma; 1:20,000); Na<sup>+</sup>/K<sup>+</sup> ATPase (Novus; 1:3000); Calnexin (Abcam; 1:5000); Flag (Sigma; 1:10,000); Myc (Roche; 1:1000); p-AKT (Ser473) (Cell Signaling; 1:1000); AKT (Santa Cruz; 1:4000); p-ERK1/2 (Cell Signaling; 1:2000); ERK1/2 (Cell Signaling; 1:2000); p-MYPT1 (Thr696) (EMD Millipore; 1:2000); MYPT1 (Cell Signaling; 1:2000); p-MLC2 (Ser19) (Cell Signaling; 1:1000); MLC2 (Cell Signaling; 1:2000).

### Quantitative Real-Time PCR Assays

Total RNA was prepared with the RNeasy Kit (Qiagen). cDNA was prepared using a TaqMan reverse transcription kit, and real-time PCR was performed with TaqMan PCR mixture (Applied Biosystems, Foster City, CA) according to standard protocols<sup>21</sup>. The Taqman primers for human *ROCK1* (Hs01127699\_m1), human *ROCK2* (Hs00178154\_m1), human *actin* (Hs99999903\_m1), mouse *ROCK1* (Mm00485745\_m1), mouse *ROCK2* (Mm01270843\_m1) and mouse *actin* (Mm01205647\_g1) were purchased from Applied Biosystems. The expression of *ROCK1* and *ROCK2* in cells was normalized to the expression of *actin* gene.

### Assays for RhoA and ROCK activities

For RhoA activity analysis, GST-Rhotekin Rho binding domain (RBD) pull-down assays were performed with Rho activity kits (Millipore) to measure the levels of GTP-bound RhoA (RhoA-GTP) in cells<sup>59</sup>. The RBD of the Rho effector protein Rhotekin binds specifically to the RhoA-GTP. The levels of precipitated RhoA-GTP were measured by Western-blot assays using a RhoA antibody, and normalized to total RhoA levels in cells. The ROCK activity was measured by enzyme immunoassays using ROCK activity assay kits (Millipore). In brief, ROCK1 and ROCK2 (ROCK1/2) were immunoprecipitated from cell lysates and added to 96-well plates pre-coated with recombinant MYPT1, which contains a Thr696 residue that can be phosphorylated by ROCK1/2<sup>59</sup>. The levels of MYPT1 phosphorylation on Thr696, which represent the ROCK1/2 activities, were detected with a phospho-MYPT1-Thr696 antibody (1:1000) and an HRP-conjugated secondary detection antibody (1:2000).

### Analysis of endogenous levels of GLUTs on the PM

The PM fraction of cells was isolated according to standard protocols<sup>60, 61</sup>. Briefly, the PM fraction was separated from the other membrane fraction of cells which includes the endoplasmic reticulum (ER). The expression levels of GLUT1, 2 and 3 in PM fraction were measured by Western-blot assays. A PM protein Na<sup>+</sup>/K<sup>+</sup> ATPase was detected as an internal standard. Calnexin, an ER membrane protein, was detected to exclude the contamination of PM by the other membrane fraction which includes the ER. The whole cell extracts were used to measure the total GLUT1, 2 and 3 in cells.

### Analysis of the levels of Myc tagged GLUTs on the PM

The pEGP-Myc-GLUT1 and pcDNA3-Myc-GLUT2 vectors which express GLUT1 and GLUT2 with Myc tag in their first exofacial loops, respectively, (generous gifts from Dr. Jeffrey Pessin), were used to construct pLPCX-Myc-GLUT1 and 2 vectors, respectively. pLPCX-Myc-GLUT3 vector expressing GLUT3 with Myc tag in its first exofacial loop was constructed by PCR amplification. The levels of Myc-GLUT1, 2 and 3 on the cell surface and in whole cells were measured by IF staining in a flow cytometry<sup>62, 63</sup>. Briefly, at 48 h after cells were transduced with pLPCX-Myc-GLUT1, 2, or 3 vectors, cells were blocked in PBS with 2% FBS and stained with a Myc antibody (Roche) to detect Myc-GLUT1, 2, or 3 on cell surface in a flow cytometry. To determine the total levels of Myc-GLUT1, 2 or 3 in cells, cells were fixed with 2% paraformaldehyde and permeabilized with 0.2% Triton

X-100 before staining. The relative levels of Myc-GLUT 1, 2 or 3 on cell surface were calculated after normalization with their total levels in cells. Cells transduced with empty pLPCX vectors were employed as negative controls.

### Immunofluorescence staining

Immunofluorescence (IF) staining of cells were performed according to standard protocols<sup>21, 22</sup>. In brief, cells cultured on coverslips were washed with ice-cold PBS and fixed with methanol. Cells were permeabilized with PBS containing 0.2% Triton X-100. The cells expressing Myc-GLUT1 were incubated with anti-myc antibodies (9E10, Roche; 1:100) for overnight followed by Alexa Fluor® 488-conjugated goat secondary antibody (Invitrogen; 1:200) for 1 h. The coverslips were mounted in Vectashield (Vector Laboratories) and examined by a confocal laser-scanning microscope.

### Actin polymerization assays

The polymeric actin fraction was isolated from cells according to standard protocols<sup>64</sup>. Briefly, cells were homogenized in 400 µl of lysis and F-actin stabilization buffer (50 mM PIPES at pH 6.9, 50 mM NaCl, 5 mM MgCl<sub>2</sub>, 5 mM EGTA, 5% glycerol, 0.1% NP-40, 0.1% Triton X-100, 0.1% Tween-20, 0.1% β-mercaptoethanol, 1 mM ATP, protease inhibitor cocktail) for 30 min at 37°C. Following centrifugation (2,000 rpm, 5 min), half of the supernatant was transferred and centrifuged at 100,000 ×g (60 min, 37°C) to pellet polymeric actin. The pellet containing polymeric actin was resuspended in 200 µl of ice-cold water containing 10 µM cytochalasin D. The polymeric actin samples were then diluted in 4×SDS sample buffer for Western-blot assays. A monoclonal anti-actin antibody (Sigma) was used to detect polymeric actin. The whole cell extracts from the same amount of cells used for polymeric actin fraction isolation were used for the Western-blot assays to measure the levels of total actin in cells. For treatments of actin polymerization inhibitors, cells were treated with cytochalasin D (5–20 µM) or latrunculin B (1–10 µM) for 4 h before assays. Control groups were treated with DMSO.

### Anchorage-independent growth assays

Anchorage-independent growth assays were performed in dishes coated with media containing 0.6% agarose. Cells were seeded on top of this layer in media containing 0.3% agarose. Colonies were stained and counted after 2–3 weeks. For galactose treatment, cells were cultured in media containing galactose (25 mM) but no glucose.

### Xenograft tumorigenicity assays

Seven-week-old BALB/c nu/nu male athymic nude mice (Taconic) were used for xenograft tumorigenicity assays<sup>65</sup>. Cells ( $5 \times 10^6 - 1 \times 10^7$  in 0.2 mL PBS) were injected (s.c.) into nude mice (n = 10/group). After injection, mice were examined and tumor volumes were measured 3 times/week for 3–4 weeks. Tumor volume =  $\frac{1}{2}$  (length × width<sup>2</sup>).

## Statistical analysis

The differences in tumor growth among groups were analyzed for statistical significance by ANOVA, followed by Student's *t*-tests using a GraphPad Prism software. All other *P* values were obtained using two-tailed Student *t*-tests. \*:  $p < 0.005$ ; #:  $p < 0.01$ ; ##:  $p < 0.05$ .

## Supplementary Material

Refer to Web version on PubMed Central for supplementary material.

## Acknowledgements

We thank Dr. Gigi Lozano for generously providing *p53*<sup>R172H/R172H</sup> mice, and Dr. Jeffrey Pessin for generously providing the pEGP-Myc-GLUT1 and pcDNA3-Myc-GLUT2 vectors. This work was supported by grants from the NIH (R01CA143204), NJCCR, and UMDNJ Foundation (to Z.F.), and by grants from NIH (R01CA160558) and DOD Grant (W81XWH-10-1-0435) and Ellison Medical Foundation (to W.H.). C.Z. and J. L. were supported by NJCCR postdoctoral fellowships.

## REFERENCES

1. Levine AJ, Hu W, Feng Z. The P53 pathway: what questions remain to be explored? Cell death and differentiation. 2006; 13:1027–1036. [PubMed: 16557269]
2. Vousden KH, Prives C. Blinded by the Light: The Growing Complexity of p53. Cell. 2009; 137:413–431. [PubMed: 19410540]
3. Levine AJ, Oren M. The first 30 years of p53: growing ever more complex. Nat Rev Cancer. 2009; 9:749–758. [PubMed: 19776744]
4. Stambolsky P, et al. Modulation of the vitamin D3 response by cancer-associated mutant p53. Cancer Cell. 2010; 17:273–285. [PubMed: 20227041]
5. Muller PA, et al. Mutant p53 drives invasion by promoting integrin recycling. Cell. 2009; 139:1327–1341. [PubMed: 20064378]
6. Muller PA, Vousden KH. p53 mutations in cancer. Nature cell biology. 2013; 15:2–8. [PubMed: 23263379]
7. Freed-Pastor WA, et al. Mutant p53 disrupts mammary tissue architecture via the mevalonate pathway. Cell. 2012; 148:244–258. [PubMed: 22265415]
8. Lang GA, et al. Gain of function of a p53 hot spot mutation in a mouse model of Li-Fraumeni syndrome. Cell. 2004; 119:861–872. [PubMed: 15607981]
9. Olive KP, et al. Mutant p53 gain of function in two mouse models of Li-Fraumeni syndrome. Cell. 2004; 119:847–860. [PubMed: 15607980]
10. Feng Z, Levine AJ. The regulation of energy metabolism and the IGF-1/mTOR pathways by the p53 protein. Trends Cell Biol. 2010; 20:427–434. [PubMed: 20399660]
11. Hanahan D, Weinberg RA. Hallmarks of cancer: the next generation. Cell. 2011; 144:646–674. [PubMed: 21376230]
12. Vousden KH, Ryan KM. p53 and metabolism. Nat Rev Cancer. 2009; 9:691–700. [PubMed: 19759539]
13. Levine AJ, Puzio-Kuter AM. The control of the metabolic switch in cancers by oncogenes and tumor suppressor genes. Science. 2010; 330:1340–1344. [PubMed: 21127244]
14. Warburg O. On the origin of cancer cells. Science. 1956; 123:309–314. [PubMed: 13298683]
15. Fantin VR, St-Pierre J, Leder P. Attenuation of LDH-A expression uncovers a link between glycolysis, mitochondrial physiology, and tumor maintenance. Cancer Cell. 2006; 9:425–434. [PubMed: 16766262]
16. Christofk HR, et al. The M2 splice isoform of pyruvate kinase is important for cancer metabolism and tumour growth. Nature. 2008; 452:230–233. [PubMed: 18337823]

17. Aylon Y, Oren M. New plays in the p53 theater. *Curr Opin Genet Dev.* 2011; 21:86–92. [PubMed: 21317061]
18. Li T, et al. Tumor suppression in the absence of p53-mediated cell-cycle arrest, apoptosis, and senescence. *Cell.* 2012; 149:1269–1283. [PubMed: 22682249]
19. Bensaad K, et al. TIGAR, a p53-inducible regulator of glycolysis and apoptosis. *Cell.* 2006; 126:107–120. [PubMed: 16839880]
20. Matoba S, et al. p53 regulates mitochondrial respiration. *Science.* 2006; 312:1650–1653. [PubMed: 16728594]
21. Zhang C, et al. Parkin, a p53 target gene, mediates the role of p53 in glucose metabolism and the Warburg effect. *Proc Natl Acad Sci U S A.* 2011; 108:16259–16264. [PubMed: 21930938]
22. Hu W, et al. Glutaminase 2, a novel p53 target gene regulating energy metabolism and antioxidant function. *Proc Natl Acad Sci U S A.* 2010; 107:7455–7460. [PubMed: 20378837]
23. Garcia-Cao I, et al. Systemic elevation of PTEN induces a tumor-suppressive metabolic state. *Cell.* 2012; 149:49–62. [PubMed: 22401813]
24. Fang S, et al. Corepressor SMRT promotes oxidative phosphorylation in adipose tissue and protects against diet-induced obesity and insulin resistance. *Proc Natl Acad Sci U S A.* 2012; 108:3412–3417. [PubMed: 21300871]
25. Bogan JS. Regulation of Glucose Transporter Translocation in Health and Diabetes. *Annu Rev Biochem.* 2012; 81:507–532. [PubMed: 22482906]
26. Ganapathy V, Thangaraju M, Prasad PD. Nutrient transporters in cancer: relevance to Warburg hypothesis and beyond. *Pharmacol Ther.* 2009; 121:29–40. [PubMed: 18992769]
27. Szablewski L. Expression of glucose transporters in cancers. *Biochim Biophys Acta.* 2012; 1835:164–169. [PubMed: 23266512]
28. Bentley J, et al. Interleukin-3-mediated cell survival signals include phosphatidylinositol 3-kinase-dependent translocation of the glucose transporter GLUT1 to the cell surface. *J Biol Chem.* 2003; 278:39337–39348. [PubMed: 12869574]
29. Ridley AJ. Rho GTPases and actin dynamics in membrane protrusions and vesicle trafficking. *Trends in cell biology.* 2006; 16:522–529. [PubMed: 16949823]
30. Karlsson R, Pedersen ED, Wang Z, Brakebusch C. Rho GTPase function in tumorigenesis. *Biochim Biophys Acta.* 2009; 1796:91–98. [PubMed: 19327386]
31. Sahai E, Marshall CJ. RHO-GTPases and cancer. *Nat Rev Cancer.* 2002; 2:133–142. [PubMed: 12635176]
32. Ishikura S, Koshkina A, Klip A. Small G proteins in insulin action: Rab and Rho families at the crossroads of signal transduction and GLUT4 vesicle traffic. *Acta Physiol (Oxf).* 2008; 192:61–74. [PubMed: 18171430]
33. Standaert M, et al. Comparative effects of GTPgammaS and insulin on the activation of Rho, phosphatidylinositol 3-kinase, and protein kinase N in rat adipocytes. Relationship to glucose transport. *J Biol Chem.* 1998; 273:7470–7477. [PubMed: 9516446]
34. Bossi G, et al. Conditional RNA interference in vivo to study mutant p53 oncogenic gain of function on tumor malignancy. *Cell Cycle.* 2008; 7:1870–1879. [PubMed: 18594199]
35. Muller PA, Vousden KH, Norman JC. p53 and its mutants in tumor cell migration and invasion. *J Cell Biol.* 2011; 192:209–218. [PubMed: 21263025]
36. Mizuarai S, Yamanaka K, Kotani H. Mutant p53 induces the GEF-H1 oncogene, a guanine nucleotide exchange factor-H1 for RhoA, resulting in accelerated cell proliferation in tumor cells. *Cancer Res.* 2006; 66:6319–6326. [PubMed: 16778209]
37. Timpson P, et al. Spatial regulation of RhoA activity during pancreatic cancer cell invasion driven by mutant p53. *Cancer research.* 2011; 71:747–757. [PubMed: 21266354]
38. Jaffe AB, Hall A. Rho GTPases: biochemistry and biology. *Annu Rev Cell Dev Biol.* 2005; 21:247–269. [PubMed: 16212495]
39. Chun KH, et al. Regulation of glucose transport by ROCK1 differs from that of ROCK2 and is controlled by actin polymerization. *Endocrinology.* 2012; 153:1649–1662. [PubMed: 22355071]
40. Furukawa N, et al. Role of Rho-kinase in regulation of insulin action and glucose homeostasis. *Cell Metab.* 2005; 2:119–129. [PubMed: 16098829]

41. Lee DH, et al. Targeted disruption of ROCK1 causes insulin resistance in vivo. *J Biol Chem.* 2009; 284:11776–11780. [PubMed: 19276091]
42. Ishizaki T, et al. Pharmacological properties of Y-27632, a specific inhibitor of rho-associated kinases. *Molecular pharmacology.* 2000; 57:976–983. [PubMed: 10779382]
43. Vivanco I, Sawyers CL. The phosphatidylinositol 3-Kinase AKT pathway in human cancer. *Nat Rev Cancer.* 2002; 2:489–501. [PubMed: 12094235]
44. Roberts PJ, Der CJ. Targeting the Raf-MEK-ERK mitogen-activated protein kinase cascade for the treatment of cancer. *Oncogene.* 2007; 26:3291–3310. [PubMed: 17496923]
45. Wong KK, Engelman JA, Cantley LC. Targeting the PI3K signaling pathway in cancer. *Current opinion in genetics & development.* 2010; 20:87–90. [PubMed: 20006486]
46. Hanel W, et al. Two hot spot mutant p53 mouse models display differential gain of function in tumorigenesis. *Cell death and differentiation.* 2013; 20:898–909. [PubMed: 23538418]
47. Clemmons DR. Modifying IGF1 activity: an approach to treat endocrine disorders, atherosclerosis and cancer. *Nature reviews. Drug discovery.* 2007; 6:821–833. [PubMed: 17906644]
48. Lanzetti L. Actin in membrane trafficking. *Curr Opin Cell Biol.* 2007; 19:453–458. [PubMed: 17616384]
49. Maekawa M, et al. Signaling from Rho to the actin cytoskeleton through protein kinases ROCK and LIM-kinase. *Science.* 1999; 285:895–898. [PubMed: 10436159]
50. Wakatsuki T, Schwab B, Thompson NC, Elson EL. Effects of cytochalasin D and latrunculin B on mechanical properties of cells. *Journal of cell science.* 2001; 114:1025–1036. [PubMed: 11181185]
51. Goddette DW, Frieden C. Actin polymerization. The mechanism of action of cytochalasin D. *J Biol Chem.* 1986; 261:15974–15980. [PubMed: 3023337]
52. Finley LW, et al. SIRT3 opposes reprogramming of cancer cell metabolism through HIF1alpha destabilization. *Cancer cell.* 2011; 19:416–428. [PubMed: 21397863]
53. Weinberg F, et al. Mitochondrial metabolism and ROS generation are essential for Kras-mediated tumorigenicity. *Proc Natl Acad Sci U S A.* 2010; 107:8788–8793. [PubMed: 20421486]
54. Freed-Pastor WA, Prives C. Mutant p53: one name, many proteins. *Genes & development.* 2012; 26:1268–1286. [PubMed: 22713868]
55. Hu W, Feng Z, Teresky AK, Levine AJ. p53 regulates maternal reproduction through LIF. *Nature.* 2007; 450:721–724. [PubMed: 18046411]
56. Haemmerle G, et al. Defective lipolysis and altered energy metabolism in mice lacking adipose triglyceride lipase. *Science.* 2006; 312:734–737. [PubMed: 16675698]
57. Hofmann SM, et al. Adipocyte LDL receptor-related protein-1 expression modulates postprandial lipid transport and glucose homeostasis in mice. *The Journal of clinical investigation.* 2007; 117:3271–3282. [PubMed: 17948131]
58. Koivisto UM, et al. Differential regulation of the GLUT-1 and GLUT-4 glucose transport systems by glucose and insulin in L6 muscle cells in culture. *J Biol Chem.* 1991; 266:2615–2621. [PubMed: 1990010]
59. Gong H, et al. G protein subunit Galpha13 binds to integrin alphaIIb beta3 and mediates integrin "outside-in" signaling. *Science.* 2010; 327:340–343. [PubMed: 20075254]
60. Simpson IA, et al. Insulin-stimulated translocation of glucose transporters in the isolated rat adipose cells: characterization of subcellular fractions. *Biochim Biophys Acta.* 1983; 763:393–407. [PubMed: 6360220]
61. Perrini S, et al. Dehydroepiandrosterone stimulates glucose uptake in human and murine adipocytes by inducing GLUT1 and GLUT4 translocation to the plasma membrane. *Diabetes.* 2004; 53:41–52. [PubMed: 14693696]
62. Michalek RD, et al. Estrogen-related receptor-alpha is a metabolic regulator of effector T-cell activation and differentiation. *Proc Natl Acad Sci U S A.* 2011; 108:18348–18353. [PubMed: 22042850]
63. Wieman HL, Wofford JA, Rathmell JC. Cytokine stimulation promotes glucose uptake via phosphatidylinositol-3 kinase/Akt regulation of Glut1 activity and trafficking. *Molecular biology of the cell.* 2007; 18:1437–1446. [PubMed: 17301289]

64. Miyamoto K, Pasque V, Jullien J, Gurdon JB. Nuclear actin polymerization is required for transcriptional reprogramming of Oct4 by oocytes. *Genes Dev.* 25:946–958. [PubMed: 21536734]
65. Hu W, et al. Negative regulation of tumor suppressor p53 by microRNA miR-504. *Mol Cell.* 2010; 38:689–699. [PubMed: 20542001]

Author Manuscript

Author Manuscript

Author Manuscript

Author Manuscript

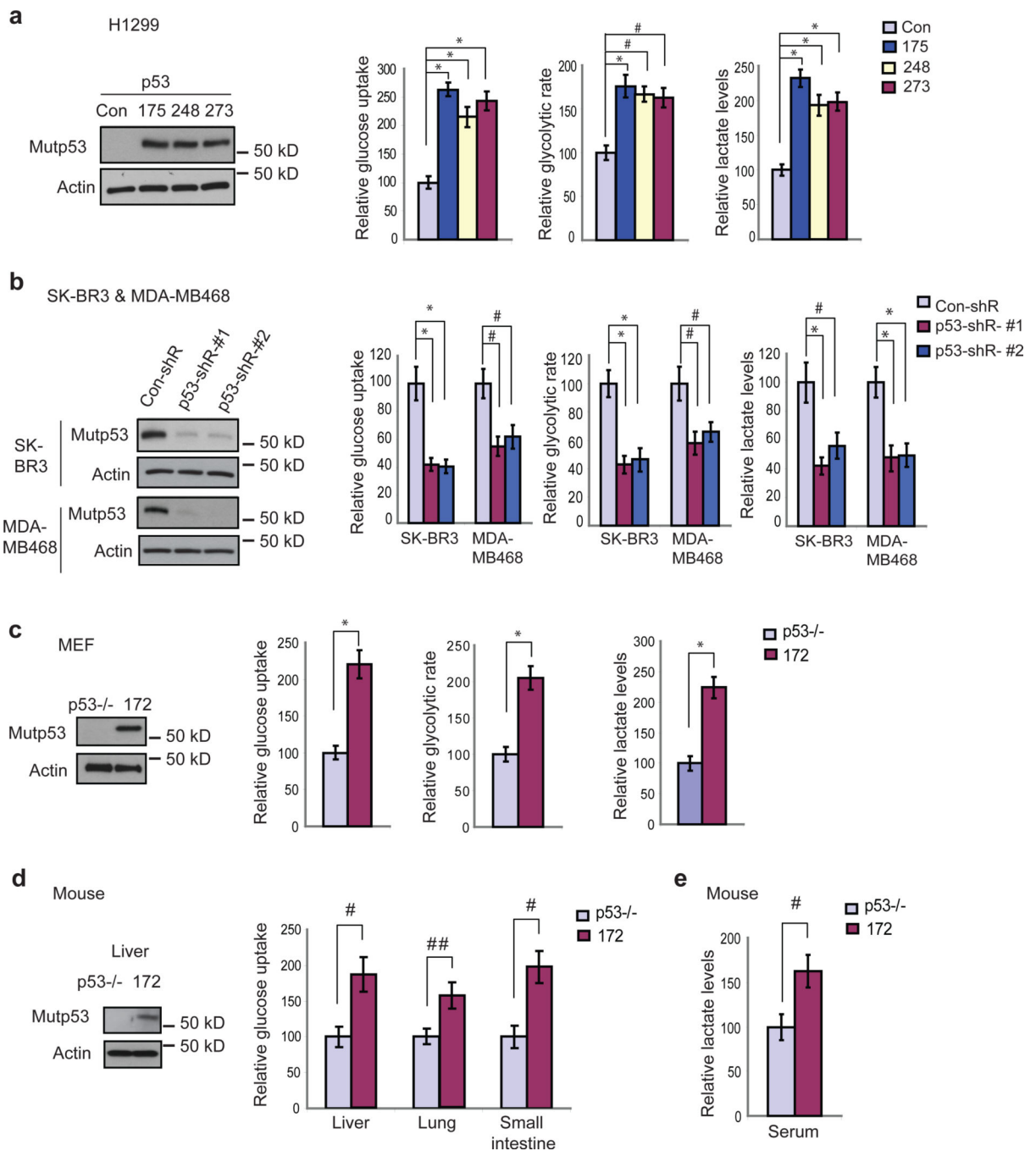


**Fig. 1. Mutp53 stimulates the Warburg effect both in vitro and in vivo**

(a) Ectopic expression of R175H, R248Q and R273H mutp53 in p53-null H1299 cells enhanced glucose uptake, glycolytic rate and lactate production. Con: Control. Left panels in a–d: mutp53 expression in cells detected by Western-blot assays. (b) Knockdown of endogenous mutp53 by two different shRNA vectors in SK-BR3 cells expressing R175H mutp53 and MDA-MB468 cells expressing R273H mutp53 reduced glucose uptake, glycolytic rate and lactate production. Con-shR: control shRNA; p53-shR: p53 shRNA. (c) Enhanced glucose uptake, glycolytic rate and lactate production in *p53*<sup>R172H/R172H</sup> MEFs

compared with  $p53^{-/-}$  MEFs. 172:  $p53^{R172H/R172H}$  **(d)** Increased glucose uptake in different tissues in  $p53^{R172H/R172H}$  mice compared with  $p53^{-/-}$  mice. **(e)** Increased serum lactate levels in  $p53^{R172H/R172H}$  mice compared with  $p53^{-/-}$  mice. Data are presented as mean  $\pm$  SD (n=5 for a-c, n=6 for d & e). ##:  $p<0.05$ ; #:  $p<0.01$ ; \*:  $p<0.005$ ; two-tailed Student *t*-test.

Author Manuscript

Author Manuscript

Author Manuscript

Author Manuscript

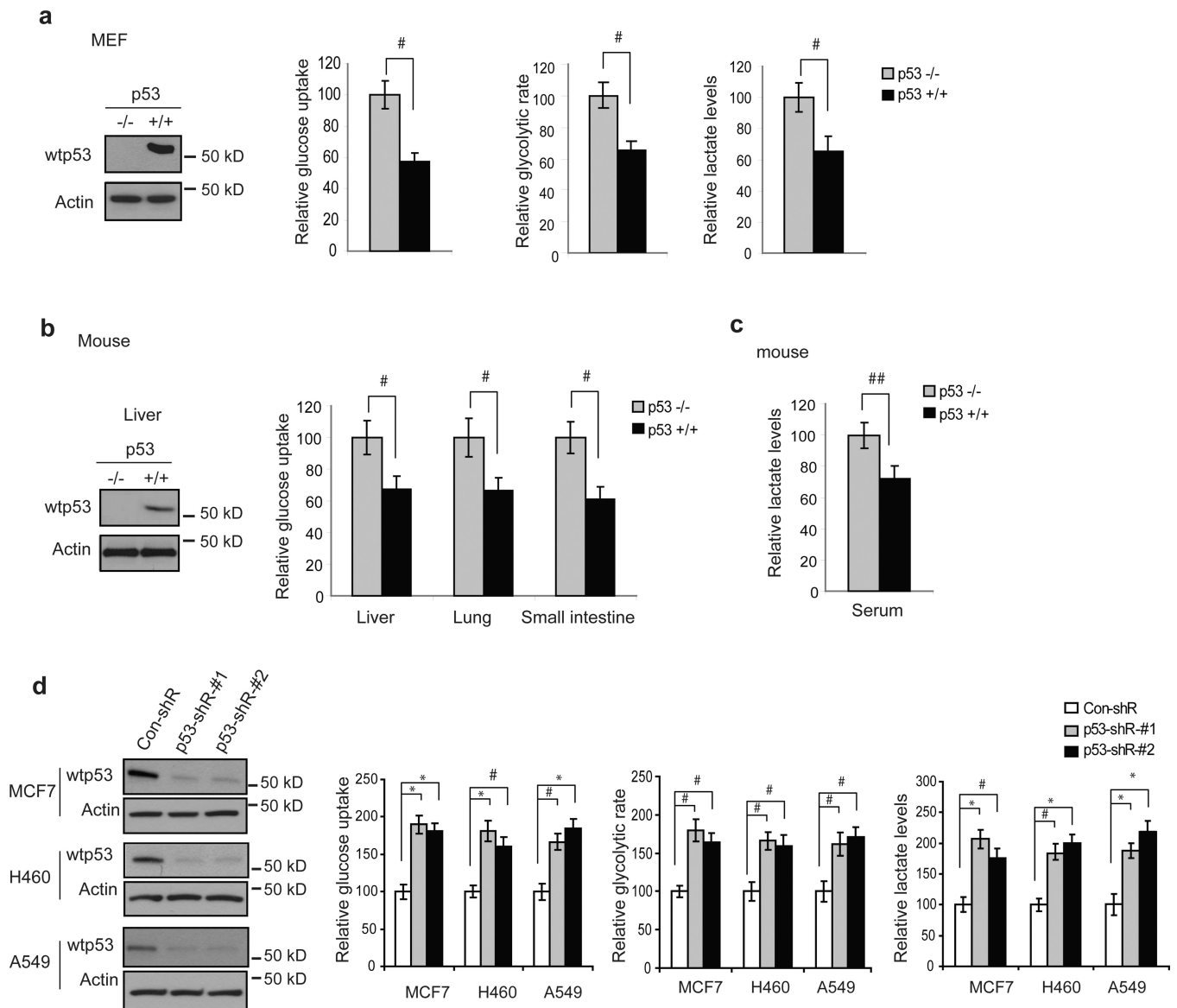


**Fig. 2. Wild type p53 inhibits the Warburg effect both *in vitro* and *in vivo***

(a) Lower levels of glucose uptake, glycolytic rate and lactate production in *p53*<sup>+/+</sup> MEF cells compared with *p53*<sup>-/-</sup> MEF cells. wtp53: wild type p53. (b) Lower levels of glucose uptake in different tissues in *p53*<sup>+/+</sup> mice compared with *p53*<sup>-/-</sup> mice. (c) Lower levels of serum lactate in *p53*<sup>+/+</sup> mice compared with *p53*<sup>-/-</sup> mice. (d) Knockdown of the endogenous wtp53 by two different shRNA vectors in human breast MCF7, human lung H460 and A549 cells which all express wtp53 enhanced glucose uptake, glycolytic rate and lactate production in cells. Con-shR: control shRNA; p53-shR: p53 shRNA. Left panels in a-d: wtp53 expression in cells detected by Western-blot assays. Data are presented as mean  $\pm$  SD (n=4 for a & d, n=6 for b & c). ##:  $p < 0.05$ ; #:  $p < 0.01$ ; \*:  $p < 0.005$ ; two-tailed Student *t*-test.

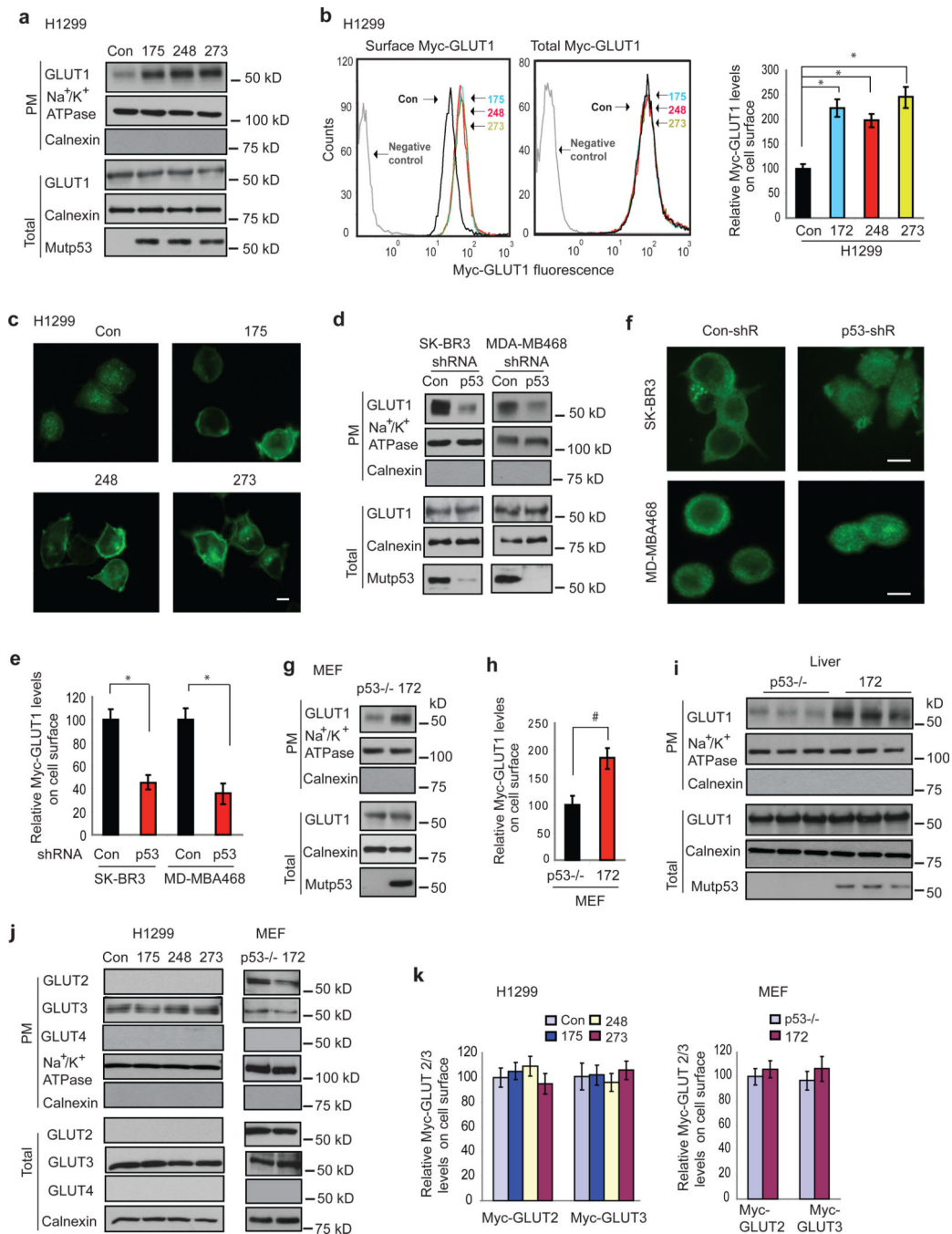


**Fig. 3. Mutp53 stimulates GLUT1 translocation to the plasma membrane both *in vitro* and *in vivo***

(a) Ectopic expression of R175H, R248Q and R273H mutp53 in H1299 cells promoted GLUT1 translocation to the plasma membrane (PM) detected by Western-blot assays. The PM protein Na<sup>+</sup>/K<sup>+</sup> ATPase acts as a loading control, and Calnexin acts as a negative control for the PM fraction. Total: whole cell lysates. (b) Mutp53 promoted Myc-GLUT1 translocation to the PM in H1299 cells analyzed in a flow cytometry. Left and middle panels: represented images of fluorescence staining of Myc-GLUT1 on cell surface (left)

and in the whole cell (middle). Right panel: relative Myc-GLUT1 levels on cell surface after normalization with the total Myc-GLUT1 levels in cells. Cells were transduced with pLPCX-Myc-GLUT1 vectors or pLPCX vectors (as negative controls) 48 h before assays. **(c)** IF staining of Myc-GLUT1 in H1299 control cells and cells with ectopic expression of R175H, R248Q or R273H mutp53. Scale bar, 10  $\mu\text{m}$ . **(d, e)** Knockdown of endogenous mutp53 by shRNA in SK-BR3 and MD-MBA468 cells reduced the translocation of endogenous GLUT1 as measured by Western-blot assays (d) and the translocation of Myc-GLUT1 to the PM measured by a flow cytometry (e). **(f)** IF staining of the Myc-GLUT1 in SK-BR3 and MD-MBA468 cells with mutp53 knockdown and control cells. Scale bar, 10  $\mu\text{m}$ . In d–f, two shRNA vectors against p53 were used and similar results were observed. **(g, h)** R172H mutp53 promoted the translocation of endogenous GLUT1 to the PM measured by Western-blot assays (g) and Myc-GLUT1 to the PM analyzed by a flow cytometry (h) in *p53*<sup>R172H/R172H</sup> MEF cells. **(i)** Higher endogenous GLUT1 levels on the PM in the liver tissues of *p53*<sup>R172H/R172H</sup> mice compared with *p53*<sup>-/-</sup> mice detected by Western-blot assays. Six mice/group were analyzed and 3 mice/group were presented. **(j)** Mutp53 did not promote the translocation or the expression of endogenous GLUT2 or GLUT3 in H1299 or MEF cells. **(k)** Mutp53 did not promote the PM translocation of Myc-GLUT2 or Myc-GLUT3 in H1299 and MEF cells analyzed by a flow cytometry. Cells were transduced with pLPCX-Myc-GLUT2 or GLUT3 vectors at 48 h before assays. Data are presented as mean  $\pm$  SD (n=4). \*:  $p < 0.005$ ; #:  $p < 0.01$ ; two-tailed Student *t*-test.

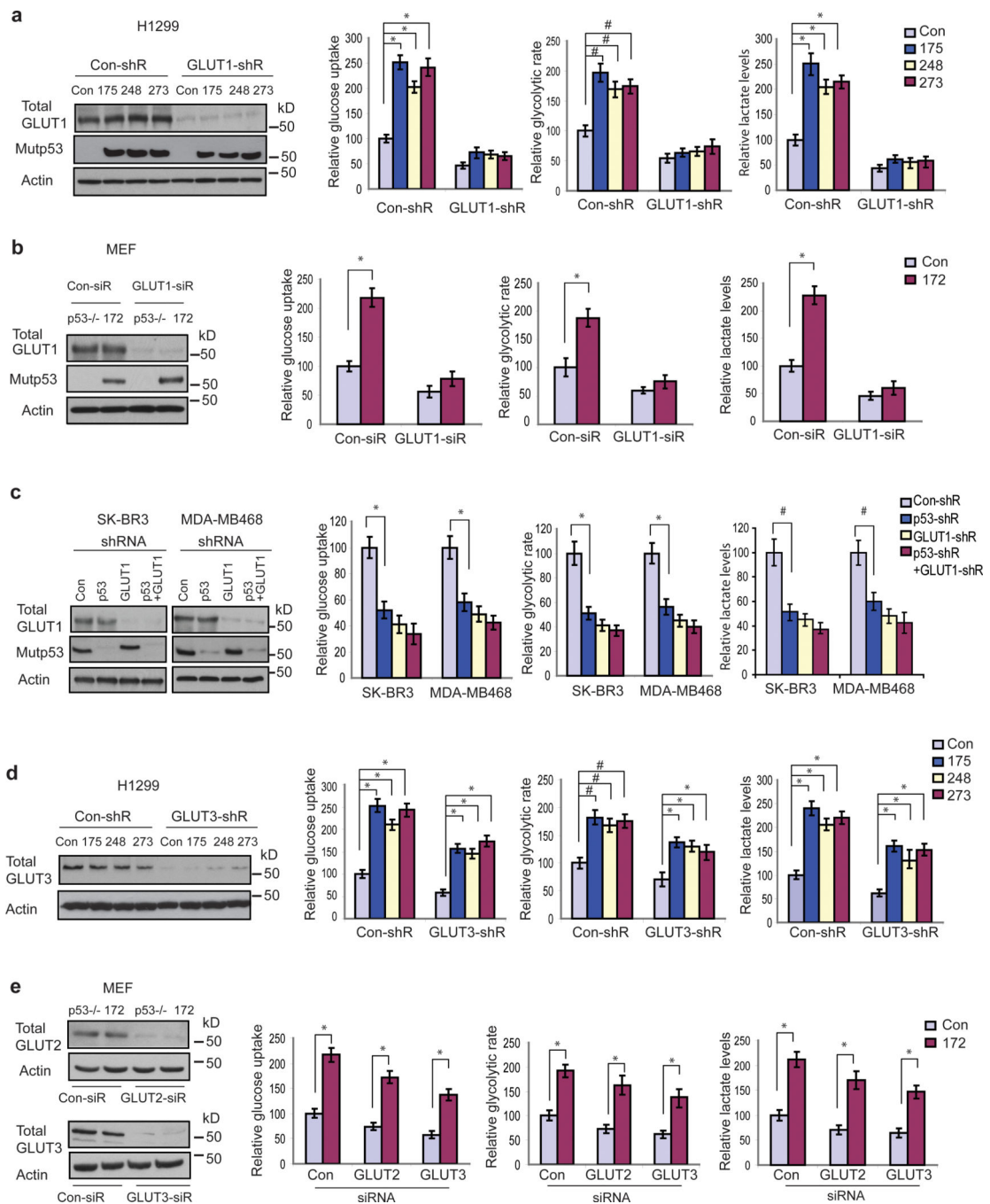


**Fig. 4. GLUT1 mediates the stimulating effect of mutp53 on the Warburg effect in cells**  
**(a)** GLUT1 knockdown by shRNA vectors largely abolished the stimulating effects of R175H, R248Q and R273H mutp53 on the Warburg effect in H1299 cells. Con-shR: Control shRNA; GLUT1-shR: GLUT1 shRNA. **(b)** GLUT1 knockdown by siRNA abolished the stimulating effect of R172H mutp53 on the Warburg effect in p53<sup>R172H/R172H</sup> MEFs. **(c)** GLUT1 knockdown by shRNA abolished the stimulating effect of R175H and R273H mutp53 on the Warburg effect in SK-BR3 and MDA-MB468 cells, respectively. **(d)** GLUT3 knockdown by shRNA did not clearly affect the stimulating effects of mutp53 on the

Warburg effect in H1299 cells. Only GLUT3 was knocked down in H1299 cells since GLUT2 expression was undetectable in H1299 (Figure 4j). (e) Knockdown of GLUT2 or GLUT3 by siRNA did not clearly affect the stimulating effect of R172H mutp53 on the Warburg effect in *p53<sup>R172H/R172H</sup>* MEFs. Left panels in a-e: knockdown of GLUT1, GLUT2, or GLUT3 in cells analyzed by Western-blot assays. Two different shRNA vectors or siRNA oligos against GLUT1, 2 and 3, respectively, were used in a-e, and similar results were observed. Data are presented as mean  $\pm$  SD (n=3). #:  $p < 0.01$ ; \*:  $p < 0.005$ ; two-tailed Student *t*-test.

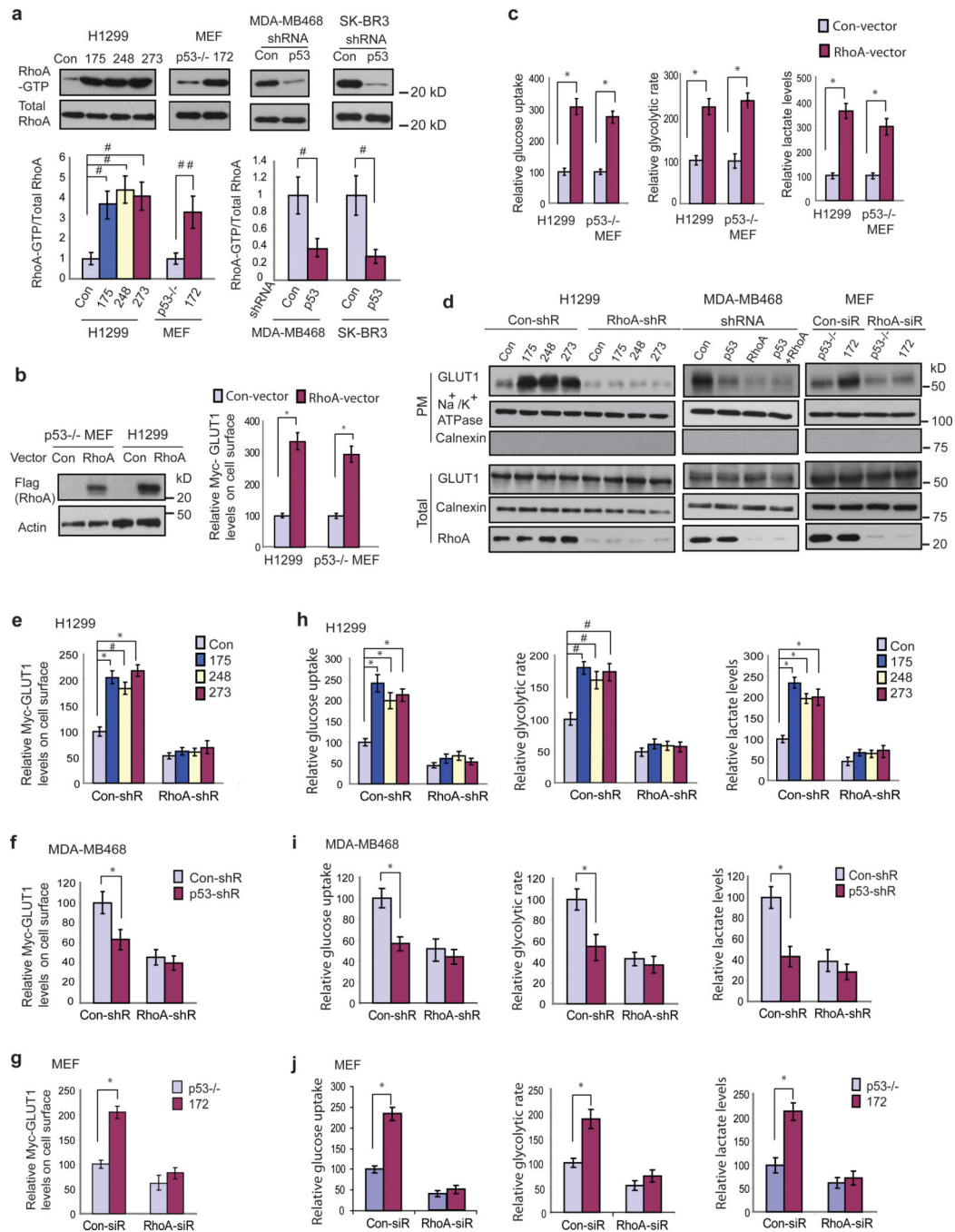


**Fig. 5. Mutp53 stimulates the Warburg effect through activating RhoA**

(a) Mutp53 enhanced RhoA activities represented by increased RhoA-GTP levels in cells. Upper panels: represented results of Western-blot assays. Lower panels: relative RhoA-GTP/total RhoA levels in cells. Data are presented as mean  $\pm$  SD (n=4). (b) Ectopic expression of RhoA by expression vectors promoted the translocation of Myc-GLUT1 to the PM in H1299 and *p53*<sup>-/-</sup> MEF cells. (c) Ectopic expression of RhoA promoted the Warburg effect in H1299 and *p53*<sup>-/-</sup> MEF cells. (d) RhoA knockdown by shRNA or siRNA largely abolished the stimulating effects of mutp53 on the translocation of

endogenous GLUT1 to the PM in H1299, MEF and MDA-MB468 cells. **(e, f, g)** RhoA knockdown largely abolished the stimulating effects of mutp53 on Myc-GLUT1 translocation to the PM in H1299 (e), MDA-MB468 (f) and MEF (g) cells. **(h, i, j)** RhoA knockdown largely abolished the stimulating effects of R273H mutp53 on the Warburg effect in H1299 (h), MDA-MB468 (i) and MEF cells (j). In d-j, two different shRNA vectors or siRNA oligos against RhoA were used and similar results were observed. Data are presented as mean  $\pm$  SD (n=4). ##:  $p < 0.05$ ; #:  $p < 0.01$ ; \*:  $p < 0.005$ ; two-tailed Student *t*-test.

Author Manuscript

Author Manuscript

Author Manuscript

Author Manuscript

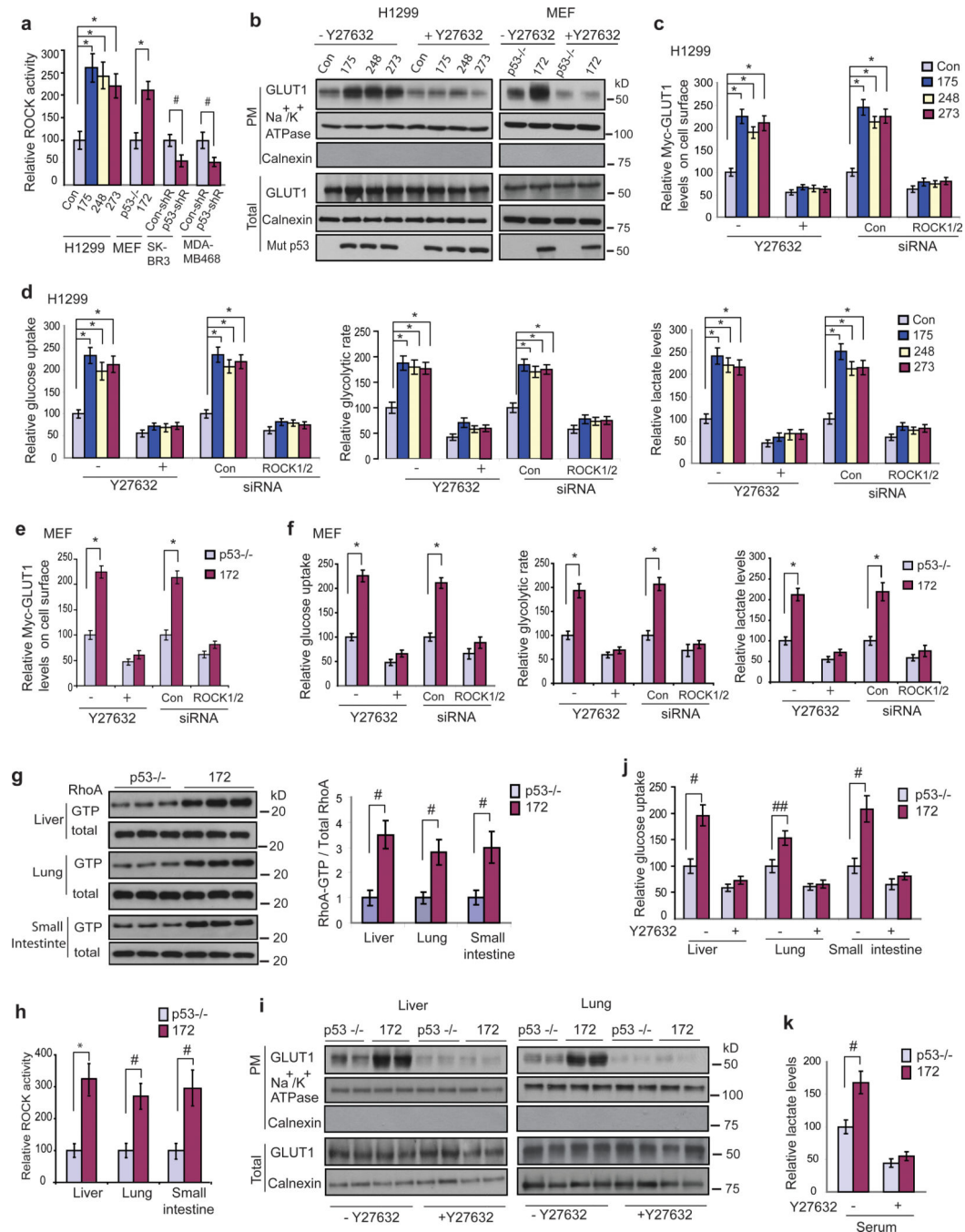


**Fig. 6. Mutp53 stimulates the Warburg effect through ROCK activation both *in vitro* and *in vivo*** (a) Mutp53 enhanced ROCK activities in H1299, MEF, SK-BR3 and MD-MB468 cells as measured by enzyme immunoassays. (b) The ROCK inhibitor Y27632 (10  $\mu$ M for 6 h) largely abolished the stimulating effect of mutp53 on GLUT1 translocation to the PM in H1299 and MEF cells. PM: plasma membrane; Total: whole cell extracts. (c, d) Y27632 treatments and ROCK1/2 knockdown by siRNA largely abolished the stimulating effects of mutp53 on Myc-GLUT1 translocation to PM (c) and the Warburg effect (d) in H1299 cells. Cells transduced with pLPCX-Myc-GLUT1 vectors were transfected with siRNA oligos to

simultaneously knock down ROCK1/2 at 24 h before assays. ROCK1/2 knockdown was confirmed by real-time PCR assays (Supplementary Fig. S5d). **(e, f)** Y27632 treatments (10  $\mu$ M for 6 h) and ROCK1/2 knockdown largely abolished the stimulating effects of mutp53 on Myc-GLUT1 translocation (e) and the Warburg effect (f) in  $p53^{R172H/R172H}$  MEF cells. **(g)** Enhanced RhoA-GTP levels in different tissues of  $p53^{R172H/R172H}$  mice compared with  $p53^{-/-}$  mice. Left panels: represented results of Western-blot assays. Right panel: relative RhoA-GTP/total RhoA levels. Data are presented as mean  $\pm$  SD (n=6 mice with two time repeats). **(h)** Increased ROCK activities in different tissues of  $p53^{R172H/R172H}$  mice compared with  $p53^{-/-}$  mice. **(i)** Y27632 largely abolished the stimulating effect of R172H mutp53 on GLUT1 translocation to PM in different mouse tissues. Mice were sacrificed at 3 h after Y27632 injection (i.p.; 10  $\mu$ g/g body weight) for assays. **(j)** Y27632 largely abolished the stimulating effect of R172H mutp53 on glucose uptake in different mouse tissues. Mice were injected (i. p.) with Y27632 at 3 h before glucose uptake assays. **(k)** Y27632 largely abolished the stimulating effect of R172H mutp53 on mouse serum lactate production. In c–f, two different siRNA oligos against ROCK1 and ROCK2, respectively, were employed and similar results were observed. In g–k, 6 mice/group were used for assays. Data are presented as mean  $\pm$  SD (n=4 in a–f and n=6 in h, j, k). ##:  $p < 0.05$ ; #:  $p < 0.01$ ; \*:  $p < 0.005$ ; two-tailed Student *t*-test.

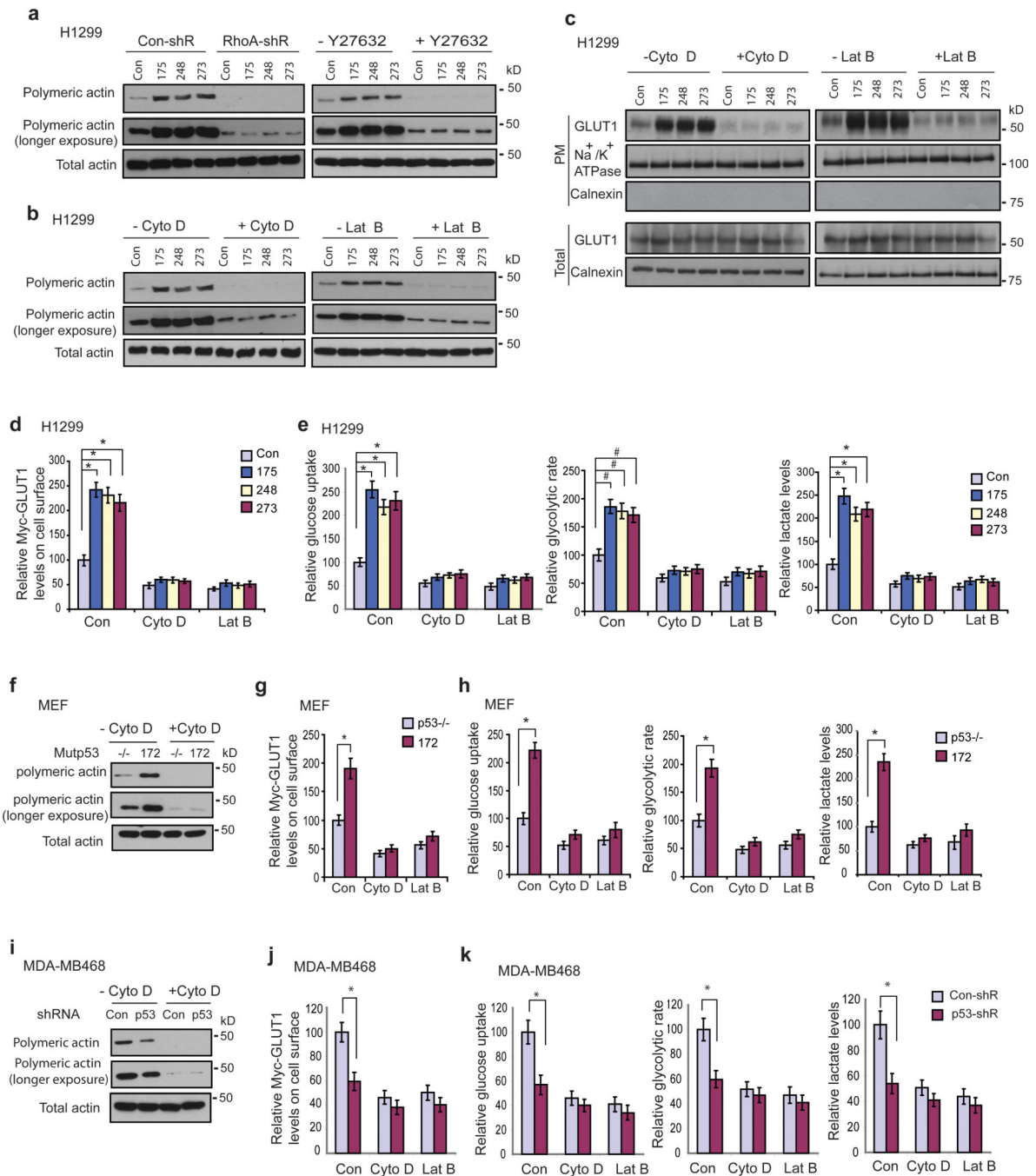


**Fig. 7. Mutp53 promotes actin polymerization to promote GLUT1 translocation to the plasma membrane**

(a) Mutp53 stimulated actin polymerization, which can be abolished by RhoA shRNA and ROCK inhibitor Y27632 (10  $\mu$ M for 6 h) in H1299 cells expressing R175H, R248Q or R273H mutp53. (b) Actin polymerization inhibitors, cytochalasin D (Cyto D) and latrunculin B (Lat B), abolished the promoting effect of mutp53 on actin polymerization in H1299 cells. (c, d) Cyto D and Lat B abolished the stimulating effect of mutp53 on the translocation of endogenous GLUT1 (c) and Myc-GLUT1 (d) to the plasma membrane (PM)

in H1299 cells. Total: whole cell extracts. **(e)** Cyto D and Lat B abolished the stimulating effect of mutp53 on the Warburg effect in H1299 cells. **(f)** Mutp53 promotes actin polymerization in *p53<sup>R172H/R172H</sup>* MEFs, which can be abolished by Cyto D. **(g, h)** Cyto D and Lat B abolished the stimulating effects of mutp53 on Myc-GLUT1 translocation to PM **(g)** and the Warburg effect **(h)** in *p53<sup>R172H/R172H</sup>* MEFs. **(i)** Knockdown of R273H mutp53 reduced actin polymerization in MDA-MB468 cells, which can be abolished by Cyto D. **(j, k)** Cyto D and Lat B abolished the stimulating effect of mutp53 on Myc-GLUT1 translocation to the PM **(j)** and the Warburg effect **(k)** in MDA-MB468 cells. Cells were treated with (+) or without (-) Cyto D (20  $\mu$ M) or Lat B (10  $\mu$ M) for 4 h before assays. Control groups (Con) were treated with DMSO. Data are presented as mean  $\pm$  SD (n=3). #:  $p < 0.05$ ; \*:  $p < 0.005$ ; two-tailed Student t-test.

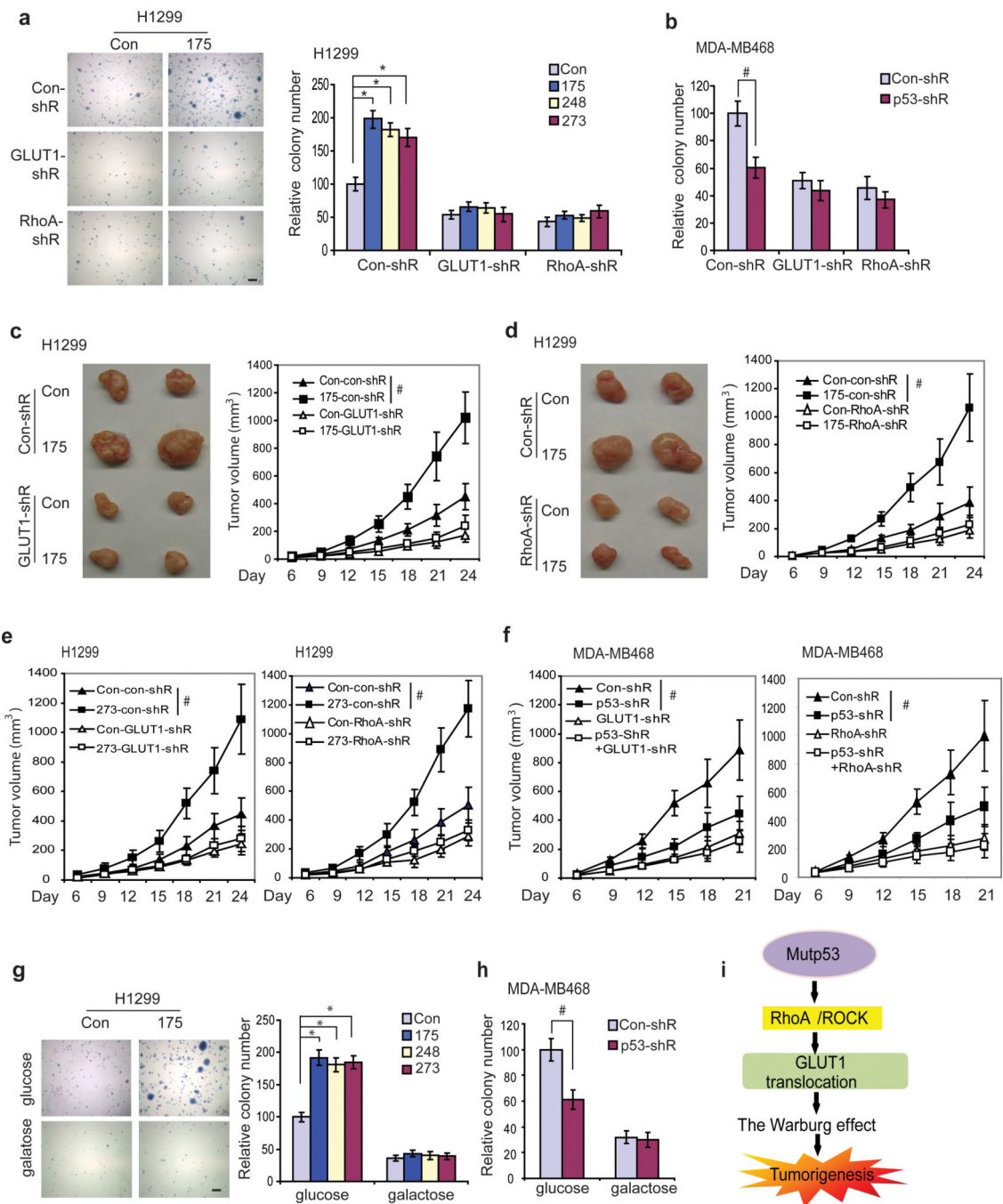


**Figure 8. Inhibition of glycolysis compromises mutp53 GOF in tumorigenesis**

(a) Knockdown of GLUT1 or RhoA by shRNA vectors (GLUT1-shR or RhoA-shR) largely abolished the promoting effects of R175H, R248Q and R273H mutp53 on the anchorage-independent growth in H1299 cells. Left panel: represented images of colonies on soft agar in H1299 cells with R175H mutp53 expression and control cells. Scale bar, 100  $\mu$ m. (b) Knockdown of GLUT1 or RhoA by shRNA vectors largely abolished the promoting effects of R273H mutp53 on the anchorage-independent growth in MDA-MB468 cells. (c, d) Knockdown of GLUT1 (c) or RhoA (d) by shRNA largely abolished the promoting effect of

R175H mutp53 on the growth of xenograft tumors in H1299 cells. Left panels: represented images of tumors on day 24. Right panels: growth curves of xenograft tumors. **(e)** Knockdown of GLUT1 (left) or RhoA (right) by shRNA largely abolished the promoting effect of R273H mutp53 on the growth of xenograft tumors in H1299 cells. **(f)** Knockdown of GLUT1 (left) or RhoA (right) by shRNA largely abolished the promoting effect of R273H mutp53 on the growth of xenograft tumors in MDA-MB468 cells. **(g, h)** Culturing cells in media containing galactose but no glucose abolished the promoting effect of mutp53 on the anchorage-independent growth in H1299 (g) and MDA-MB468 (h) cells. Left panel in (g): represented images of colonies on soft agar in H1299 cells with R175H mutp53 expression and control cells. Scale bar, 100  $\mu\text{m}$ . **(i)** Model illustrating stimulation of the Warburg effect as a novel GOF of mutp53. In a–h, two different shRNA vectors against each target gene, including GLUT1, RhoA, and p53, were employed for all assays, and similar results were observed. Data are presented as mean  $\pm$  SD (n=10 for c–f, and n=4 for the rest). \*:  $p < 0.005$ ; #:  $p < 0.01$ ; two-tailed Student *t*-test for a, b, g, and h; ANOVA followed by Student's *t*-tests for c–f.